Technical Report
TR-22-15
November 2023

Radiolysis calculations of gases in a KBS-3 canister

Jim Henshaw
Lena Z Evins

SVENSK KÄRNBRÄNSLEHANTERING AB

SWEDISH NUCLEAR FUEL
AND WASTE MANAGEMENT CO

Box 3091, SE-169 03 Solna
Phone +46 8 459 84 00
skb.se

SVENSK KÄRNBRÄNSLEHANTERING

ISSN 1404-0344
SKB TR-22-15
ID 1998630

November 2023
Updated 2025-04

Radiolysis calculations of gases in a KBS-3 canister

Jim Henshaw, Morson

Lena Z Evins, Svensk Kärnbränslehantering AB

Keywords: Radiolysis, Nitric Acid, Ammonia, Corrosion.

This report is published on www.skb.se

Update notice

The original report, dated November 2023, was found to contain both factual and editorial errors which have been corrected in this updated version. The corrected factual errors are presented below.

Updated 2025-04

Location	Original text	Corrected text
Page 51, Table 4-1:		
Case 2a, last column	2.60E–03	2.60E–02
Case 3, fifth column	310.0	320.0

Preface

The reference design on which the licensing of the KBS 3 system for the management of spent nuclear fuel is based includes a reference canister for final disposal. The reference canister, which fulfils all established design requirements for post-closure safety, consists of an outer, corrosion resistant copper shell and a load-bearing nodular cast iron insert. In SKB's continuous efforts to optimise the design of the KBS-3 repository, it is evaluated whether an alternative design of the load-bearing insert can be achieved through a simpler and more cost effective production process. As an alternative to the reference nodular cast iron insert, a design with an outer low-alloy carbon steel tube and an inner framework of carbon steel plates for either 12 BWR or 4 PWR fuel elements is being studied in the so-called Rebus project. Within the project it is evaluated if such a design has the prospects of fulfilling the same design requirements as the reference canister insert, and if this can be achieved efficiently in a full-scale production process. The Rebus insert has the same outer dimensions as the reference insert and is intended to be placed in a copper shell identical to that of the reference design.

The study documented in this report was performed to provide information that will help evaluate post-closure safety aspects of the proposed Rebus insert.

Abstract

A model has been developed to simulate the gas conditions within the KBS-3 canister which is described briefly here. The model was previously validated against experimental data and applied to the KBS-3 canister in 2021. Since 2021 some suggested change of the design parameters for the KBS-3 canister have been under discussion. These suggested changes lead to changes in surface areas, gas volumes and dose rates present in the KBS-3 canister for PWR and BWR fuel. Additionally, it has been recognised that it is valuable to use, in the model, estimated temperature evolutions that correspond to actual encapsulation scenarios. This means different temperature evolutions for BWR and PWR fuels. The KBS-3 canister gas radiolysis model has therefore been updated to reflect these changes and calculations performed for a range of possible scenarios. The details of the conditions and the results of the calculations are presented here.

The conclusions from the work are that:

- Long term redox conditions inside the canister will be reducing, the primary components produced from radiolysis being NH_3 and H_2.
- The amounts of NH_3 and H_2 in the system is a function of the initial amounts of H_2O and air.
- Increasing air at high water content leads to increased amounts of NH_3, but at low water content the amount of NH_3 in the system may decrease with increasing air content.
- Increasing dose rate leads to increased amounts of NH_3 present in the system.
- The available area for corrosion and the free gas volume in the system also impact the amount of NH_3 formed.
- For some of the scenarios investigated here NH_3 and H_2O exist simultaneously in the system, but at high relative humidity (> 60 %) the amount of NH_3 present is small.
- The length of time H_2O is present in the system is largely determined by the anaerobic corrosion rate. This therefore impacts the length of time NH_3 and H_2O exist simultaneously in the system, with low corrosion rates extending this period of time.
- If corrosion rates are low for low relative humidity (< 60 %), then oxygen is present in the system for longer and significant amounts of HNO_3 and H_2O_2 can be formed, but are destroyed by radiolysis once O_2 is consumed.
- Corrosion of the graphite seal used in the canister by gas radiolysis products will be very slow.

The assumptions used in the model are also discussed in the report however the consequences of all the assumptions have not been assessed.

Sammanfattning

En modell har tagits fram för att simulera gasförhållandena i KBS-3 kapseln som beskrivs kortfattat här. Modellen har tidigare validerats mot experimentella data och tillämpades på KBS-3-kapseln 2021. Sedan 2021 har förslag lagts fram angående ändringar av några av designparametrarna för KBS-3-kapseln, vilket leder till förändringar i ytareor, gasvolymer och doshastigheter för PWR- och BWR-kapslar. Den aktuella modelleringen har också tagit hänsyn till förväntade egenskaper hos det inkapslade bränslet vid inkapslingstillfället, vilket har lett till att andra temperaturer har använts än i tidigare modell. Modellen för beräkning av gasradiolys i förslutna KBS-3 kapslar har därför uppdaterats för att återspegla dessa förändringar och beräkningar är utförda för en rad möjliga situationer. Detaljerna om förhållandena och resultaten av beräkningarna presenteras i denna rapport.

Slutsatserna är att:

- De primära komponenterna som produceras av radiolys är NH_3 och H_2 vilket leder till en reducerande miljö inne i den förslutna kapseln.
- Mängderna av NH_3 och H_2 i systemet är en funktion av de initiala mängderna av vatten och luft.
- Ju mer luft som finns initialt, desto större mängd NH_3 bildas. Detta gäller dock inte vid låg vattenhalt då mängden NH_3 i systemet kan minska med ökande lufthalt.
- Högre doshastighet leder till ökade mängder NH_3 i systemet
- Den tillgängliga ytan för korrosion och den fria gasvolymen i systemet påverkar också mängden NH_3 som bildas.
- För några beräkningsfall finns NH_3 och vatten samtidigt i systemet, men vid hög relativ luftfuktighet (>60 %) är mängden NH_3 liten.
- Hur lång tid vatten finns i systemet bestäms till stor del av den anaeroba korrosionshastigheten. Låga korrosionshastigheter förlänger tidsperioden då NH_3 och vatten existerar samtidigt i systemet.
- De korrosiva ämnen som bildas via gasradiolys förväntas inte degradera den grafitpackning som kan bli aktuell för insatsen signifikant.

De antaganden som används i modellen diskuteras också i rapporten, men konsekvenserna av alla antaganden har inte bedömts.

Contents

1 Introduction

The KBS-3 canister will be used to store both PWR and BWR fuel assemblies for long term geological disposal. The reference KBS-3 design (SKB 2010) consists of a copper overpack covering a carbon steel and cast-iron inner container, called the insert. The insert provides structural support, while the corrosion-resistant copper cover constitutes the primary barrier to ingress of external ground water. The insert is closed with a screw fitted lid with a gas seal to isolate the gas in the insert from the gap between the insert and the copper overpack. The copper overpack is sealed using friction stir welding.

Even if the fuel is appropriately dried before encapsulation, it cannot be excluded that some water will be transferred into the canister along with the fuel. Some parts of the fuel may be difficult to dry; this is especially the case for fuel with failed cladding. It is also assumed that although the free gas volume within the canister is filled with argon, some fraction of air will remain. The gas seal separating the insert and the copper overpack is not intended for long term service. The main assumption is therefore that both container materials are exposed to the encapsulated gas mixture, although it is probable that the seal will function for (much) longer than is required. It is known that irradiation of moist air can lead to the production of aggressive reagents, such as nitric acid, and in conjunction with anoxic Fe corrosion also ammonia can form. Some of the species formed can cause stress corrosion cracking of steels and copper components (Marsh 1990). It is therefore important to understand the chemical conditions prevailing inside the canister.

To simulate the gas conditions within the KBS-3 canister, a model was developed by Henshaw and Spahiu (2021), which is described briefly below. This model was built on early assessment work performed on the gas phase conditions inside the Advanced Cold Process Canister (ACPC), an early version of the KBS-3 canister (Henshaw et al. (1990) and Henshaw (1994). The new model updated the relevant gas phase radiolysis chemistry, included the presence of a liquid water phase and accounted for the effects of steel corrosion on the gas phase chemistry. The model was then validated against experimental data and applied to the KBS-3 canister for a range of potential conditions.

Since the work reported by Henshaw and Spahiu (2021), some changes to the KBS-3 canister insert design have been explored. The main suggested change is to replace the cast iron insert with a carbon steel tube surrounding a carbon steel framework. This leads to changes in surface areas, gas volumes and dose rates present in the canister. Since all of these terms will depend on the design, burnup, and storage time of the fuel and will be different for PWR and BWR fuel assemblies, this is considered in the current calculations. It has also been recognised that, with these alternative design parameters, the temperature in the canister will be higher than previously modelled and different for each type of reactor fuel, so a single temperature profile, as used previously, is not appropriate for all canister conditions. The model has been modified to account for the new design parameters and calculations performed for both PWR and BWR fuel inserts. The details of the conditions and the results of the calculations are presented here. These results are compared to those from the previous work (Henshaw and Spaihu 2021) and discussed in detail.

The work reported here primarily focusses on the gas phase chemistry conditions within the canister, but during the project several questions arose about possible other effects of the radiation chemistry. One such question was whether any of the gas radiolysis products in the system could lead to degradation of the graphite seal used on the lid of the inner canister. Since this is a radiation chemistry topic a brief discussion of this question is given in this report.

Chapter 2 gives a brief description of the current model. Chapter 3 describes the different initial canister conditions that are modelled here and presents the results of the calculations for the various scenarios. Chapter 4 is a discussion of the results and Chapter 5 is the summary and conclusions.

2 Brief description of KBS-3 radiolysis model

A detailed description of the model used for the work presented here is given in Henshaw and Spahiu (2021) so only a short summary is provided here.

The model consists of three components:

1. Radiolysis chemistry of gaseous Ar/Air/Water mixtures leading to nitric acid and ammonia formation.
2. Vaporisation and condensation of water in the system.
3. Aerobic and anaerobic corrosion of steel components present in the system.

The radiolysis chemistry includes the primary interactions of the radiation with the gas components, for example:

$$N_2 \xrightarrow{Rad} N_2^+, N^+, e^-, N, N_2^* \quad (2\text{-}1)$$

and subsequent secondary processes in which the primary species react with each other to give the final products, for example:

$$N + O_2 \rightleftharpoons NO + O \quad (2\text{-}2)$$

$$NO + O + M \leftrightharpoons NO_2 + M \quad (2\text{-}3)$$

$$OH + NO_2 + M \leftrightharpoons HNO_3 + M \quad (2\text{-}4)$$

Here M is any other gaseous species (third body) in the system, most likely Ar for the present problem. A set of ordinary differential equations representing the gas phase chemical kinetics is solved in the model. These equations are of the form, for example for reaction (2-2),

$$\frac{d[N]}{dt} = -k_f[N][O_2] + k_r[NO][O] \quad (2\text{-}5)$$

The forward (k_f) or reverse (k_r) rate constant is often of the Arrhenius form:

$$k = AT^n \exp\left(-\frac{E}{T}\right) \quad (2\text{-}6)$$

where T is the temperature and the constants A, n and E have to be determined experimentally. Knowing either rate constant means the other can be calculated from the known thermodynamics/equilibrium constant for the reaction. The sources of the various chemical parameters are discussed in Henshaw and Spahiu (2021).

For evaporation/condensation the following reaction is included in the model:

$$H_2O(l) \rightleftharpoons H_2O(g) \quad (2\text{-}7)$$

where *(l)* is the liquid and *(g)* the gaseous state of water. The associated differential equation is simply:

$$\frac{d[H_2O]_g}{dt} = k_e([H_2O]_{eq} - [H_2O]_g) \quad (2\text{-}8)$$

Here $[H_2O]_{eq}$ is the equilibrium concentration (vapour pressure) of water at the system temperature and the constant k_e represents the rate of condensation/evaporation. In the model k_e is chosen so that $\frac{d[H_2O]_g}{dt} \cong 0$, that is $[H_2O]_{eq} \cong [H_2O]_g$, provided liquid water is present and evaporation stops if no liquid water is present.[1]

[1] It should be noted that radiolysis removes water, two pathways for which include $Ar^+ + H_2O = ArH^+ + OH$ and $Ar^+ + H_2O = Ar + H_2O^+$, subsequent neutralisation of which gives $H_2O^+ + e^- = H + OH$. At high water content primary interactions of the radiation with the water also become more important.

Aerobic (oxygen present) and anaerobic (no oxygen) steel corrosion are both modelled according to the reactions:

$$4Fe + 2H_2O + 3O_2 = 4FeOOH \quad (2\text{-}9)$$

$$3Fe + 4H_2O = Fe_3O_4 + 4H_2 \quad (2\text{-}10)$$

Aerobic corrosion consumes both O_2 and H_2O, while anaerobic corrosion consumes H_2O and generates H_2. The corrosion rates used in the model are based on a number of experimental studies (see Henshaw and Spahiu 2021). However, the overall rate of consumption of O_2 and H_2O, as well as the generation of H_2, depend on the available surface area of steel in the system, which is accounted for in the model.

The model makes a number of assumptions:

a) It ignores the radiolysis chemistry taking place in the liquid water.

b) It ignores partitioning of species such as NH_3 between the gaseous and liquid phases, if a liquid phase is present.

c) It assumes no mass transfer limitations on the movement of, for example, O_2, to steel surfaces.

d) It assumes all parts of the gas in the system are at the same temperature and subject to the same radiation dose rate, that is, the gaseous system is homogeneous.

These assumptions are discussed further in Henshaw and Spahiu (2021).

Even with these simplifying assumptions the problem still requires the solutions of several hundred simultaneous ordinary differential equations in time. These are solved with an initial set of starting conditions, these are essentially defined by the particular Case conditions, discussed below. The numerical integration package FACSIMILE was used (Curtis and Sweetenham 1987) to solve the equations. This is particularly suited to "stiff" differential equations in which the time parameters associated with the problem may vary on several different time scales. In the present case the gas radiation interactions are on the 10^{-4} s time scale, the gas chemistry on the 10^{-3} s time frame, corrosion on a 10^{7} s time scale and the behaviour of the whole system is of interest on a 10^{10} s time scale.[2] Even with a robust numerical integration tool a number of convergence problems had to be overcome for some of the calculations presented here.

[2] In general the calculations presented here indicate steady state conditions by 10^{10}s.

3 Application of the KBS-3 canister radiolysis model

3.1 Definition of initial canister conditions – Calculation cases/scenarios

The following information is required for the calculations:

- Gas temperature.
- Initial gas pressure and composition.
- Dose rate to the gas phase.
- Initial water content of the canister.
- Gas volume and available area for corrosion.

The KBS-3 canister temperature evolution during the first centuries after encapsulation is important for the model since many of the chemical rate constants are temperature dependent. Likewise, the equilibrium vapor pressure of water varies with temperature and this is also used in the model. Henshaw and Spahiu (2021) discussed a thermal analysis of the canister that had been performed for BWR fuel and temperatures were reported by (SKB 2006). Figure 3-1 is taken from this reference.

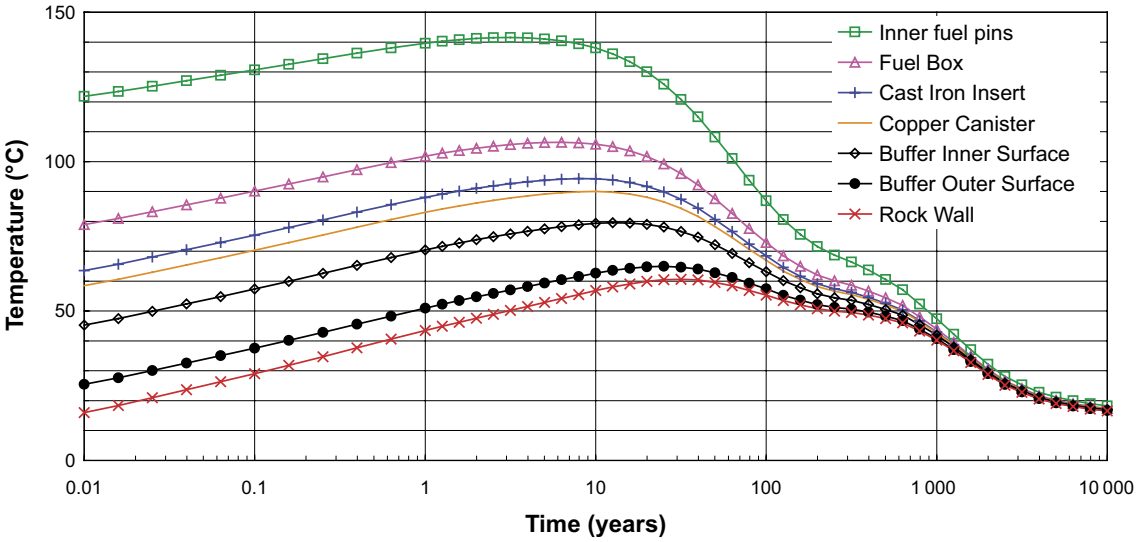

Figure 3-1. *Temperature – time evolution of various components of the KBS-3 canister, taken from (SKB 2006).*

Based on this analysis the previous work (Henshaw and Spahiu 2021) used the following temperature profile for all their calculations, as shown in Figure 3-2.

This is an average of the fuel box and insert temperatures and was implemented explicitly in the model.

However, for the suggested alternative KBS-3 design higher temperatures have been calculated[3], which leads to higher initial temperatures used in the current calculations. The initial temperatures used are 85 °C and 110 °C for BWR and PWR fuel inserts, respectively. These values correspond to estimated temperatures between the fuel and the insert at the time of encapsulation. It is assumed that the temperature increase for the first ca 10 years mimics that in Figure 3-2 and once the canisters start to cool down the curves converge after a few decades. For these two cases the temperature profiles given in Figure 3-3 were used in the current model.

It should be noted that even though the results are not very sensitive to the temperature, a few PWR calculation cases were performed using a lower initial temperature to allow initial liquid water in the canister. As is seen in Figure 3-3, in the PWR case the temperature does not go below 100 °C until after a couple of decades.

The system pressure is assumed to start at 1 atm, meaning under PWR fuel conditions all the water is in the vapour phase and remains so for over 10 years, while for BWR fuel the temperature does not rise above 100 °C for several months after encapsulation, so initially liquid water may be present in the system.

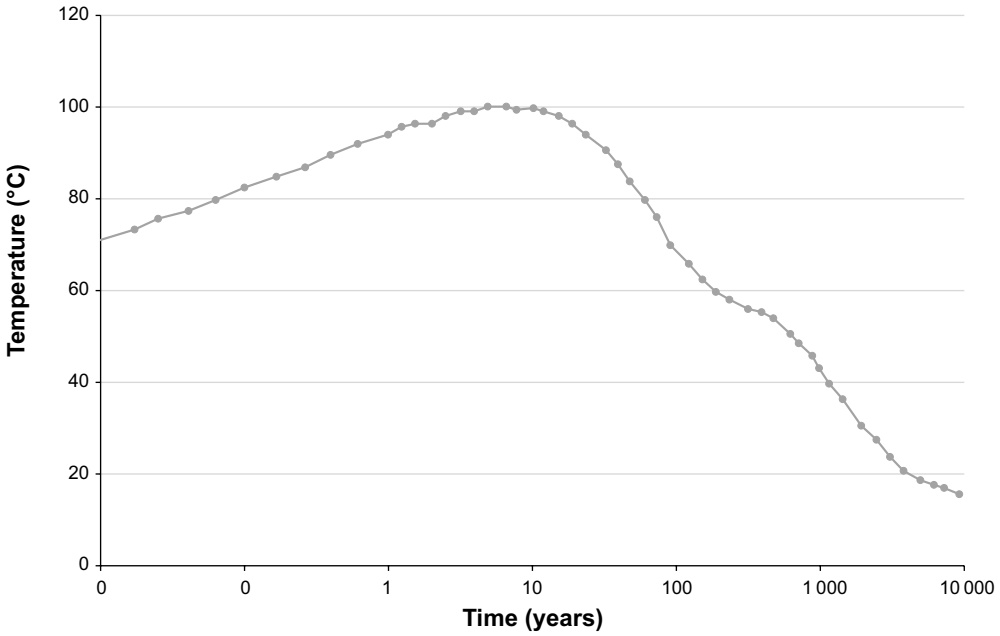

Figure 3-2. *Temperature – time evolution used in the previous version of the model.*

[3] SKB 2023. Post-closure safety evaluations of alternative KBS-3 canister insert designs. Interim version. SKBdoc 1969342 ver 1.0, Svensk Kärnbränslehantering AB. (Internal document.)

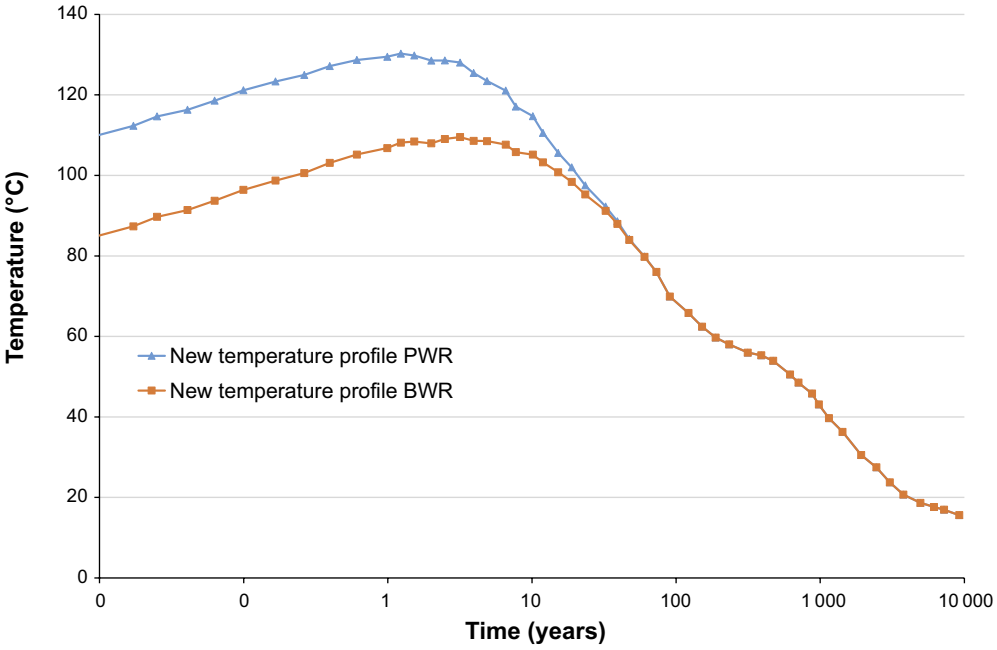

Figure 3-3. *Temperature – time evolution used in the current model.*

The dose rates used in the model are expressed by the following equation:[4]

$$D = D_o \exp(-kt) \quad (3\text{-}1)$$

where D_0 is the initial canister dose rate and the decay constant k is 7.3×10^{-10} s^{-1}, giving a dose rate half-life of approximately 30.1 years.[5] The dose rate depends on characteristics of the encapsulated spent fuel and so there will be some variation between canisters. The type of fuel (BWR or PWR), burnup and decay time since removed from the reactor will vary between individual fuel assemblies, which will influence any particular dose rate. In the previous calculations of Henshaw and Spahiu (2021) a value of D_0 of 310 Gy/h was used; this dose rate is consistent with fuel with only 1–5 years cooling time. For the current report, this dose rate has been re-assessed to better reflect expected dose rates from Swedish encapsulated fuel. Dose rates to gas between the fuel rods were calculated by Loberg (2023), providing initial low and high dose rates for BWR and PWR fuel in a KBS-3 canister with an alternative, carbon steel insert. The revised initial dose rates for the current study change the BWR values to 39 and 166 Gy/h; for PWR: 57 and 238 Gy/h. These initial dose rates correspond to fuel assemblies with 20 to 60 years cooling time, with burnups ranging from 30 to 55 MWd/kgU. Thus, these dose rates correspond to expected minimum and maximum dose rates to gas between the fuel pins in individual encapsulated fuel assemblies according to SKB's current encapsulation simulation.[6]

A free gas volume of 1 m^3 and surface area of 35 m^2 for the internal steel was previously used in calculating the gas consumption and production rates from corrosion (SKB 2010). The alternative carbon steel inserts relevant for the current report have different geometries and therefore also different free gas volumes and surface areas. The new values used are 1.25 m^3, 68.78 m^2 (BWR), 1.44 m^3, 42.52 m^2 (PWR). These values are based on internal area and volume (Ronneteg 2023), to which are added the steel area and volume between the copper shell and the steel tube. Finally, the fuel displacement volume is subtracted from the volume to get the free volume. The larger surface

[4] The dose rate is predominantly gamma and is discussed in Henshaw and Spahiu (2021). However, for gases the radiation type is much less important than for liquids and solids.

[5] The dose rate half-life up to 500 y is primarily controlled by Cs-137 after which it decays less rapidly, most of the calculations present here are up to 500 y.

[6] SKB, 2021. Använt kärnbränsle att hantera i KBS-3-systemet. SKBdoc 1380282 ver 3.0, Svensk Kärnbränslehantering AB, (Internal document, in Swedish.)

areas compared to previous calculations will increase the rate of consumption of O_2 and H_2O by corrosion. These volumes and areas include the outer part of the insert and the gas volume between the steel insert and the copper overpack since the gasket between the lid and main body of the insert is not required to be tight for more than 72 hours. However, since it is likely that the gasket will be intact for much longer, a few calculations are also performed for volumes and areas of only the inner parts of the insert.

Calculations were performed for a range of KBS-3 canister water masses and gas compositions. The maximum water content studied here was 600 g, which corresponds to 12 leaking fuel rods within the canister containing 50 g of water each (Neretnieks and Johansson 2014). This is a very pessimistic assumption. A more realistic case is 30 g of water, corresponding to residual water in a canister with only a few leaking fuel rods that have been vacuum dried with some added heat (Spahiu 2021). The main gas component is Ar with small amounts of air. For the calculations performed here gas mixtures containing initially 10 %, 5 %, 2 % and 1 % air have been considered. The reason for this variation is that 10 % is currently the level which is relevant for the post-closure safety assessment; however, a new requirement for the canister production is that air levels should be no more than 1 %.[7] How the amount of remaining air is influencing the results of the radiolysis calculations is therefore explored in the current report.

A few cases explore the effects of slowly introducing the water to the gas volume. The reason for this is the assumption that most of the encapsulated water will, at the time of encapsulation, be found within the few fuel rods with failed cladding. This water is not expected to be immediately present in the canister void, but be transferred from the rod to the void at a certain rate. The rate used in the calculations is 1.8 g/day, assuming 6 failed rods in a canister, and that water from one failed rod will be released at a rate of 0.3 g/day once the temperature in the canister reaches 120 °C (unpublished model). There are many uncertainties associated with the expected number of failed rods, expected temperature evolution and efficiency of fuel drying. Due to all these uncertainties one approximate rate was selected and was used to explore what the effect would be.

The relative humidity inside the sealed canister is also an important factor to consider. For high relative humidity, it can be assumed that corrosion rates are the same in steam and in liquid water. For low relative humidity in the gas, this may not be the case and therefore, a few cases consider a lower corrosion rate at low relative humidity.

Another uncertainty relates to area and volume, since the insert is sealed with a gasket that is assumed to fail during the timeframe relevant for the processes discussed here. However, it is possible that the seal is still intact. Thus, a few cases assume a smaller area and volume correlated to only the interior of the insert. The full range of cases are given in Table 3-1, which shows a number of scenarios where the dose rates, steel areas, gas volumes and initial temperature have been changed from the base case conditions. These calculations were performed to examine the sensitivity of the results to these input parameters as it is recognised there is some degree of uncertainty in defining the initial canister conditions.

The model has been used to calculate the production and evolution over time of H_2O, O_2, H_2, HNO_3, HNO_2, H_2O_2, N_2, and NH_3 in the system for all the cases listed in Table 3-1. The resulting data are stored as Excel files in the SKB document handling system (SKBdoc).[8]

The results from all the calculations are presented in the following sections.

[7] Tidäng J, 2022. Clink – Konstruktionsstyrande krav – Produktion och Drift. SKBdoc 1911588, ver 3.0. Svensk Kärnbränslehantering AB. (Internal document, in Swedish.)

[8] BWR Cases, SKBdoc 2002171, PWR Cases SKBdoc 2002172. (Internal documents.)

Table 3-1. All the cases that have been modelled for the current study. Base cases in bold. Changed parameters in red.

Case	Fuel type	Surface Area (m^2)	Free Volume* (m^3)	Dose rate Gy/h)	Initial Temperature (°C)	Air (%)	Initial Water in free volume(g)	Initial Water in failed rods	Water release rate from failed rods (g/day)	Corrosion Rate Oxic (mm/y)	Corrosion Rate Anoxic (mm/y)
1	BWR	68.78	1.25	39	85	10	600	N/A		0.4	3×10^{-3}
2a	**BWR**	**68.78**	**1.25**	**166**	**85**	**10**	**600**	**N/A**		**0.4**	**3×10^{-3}**
2b	BWR	54.1	1.02	166	85	10	600			0.4	3×10^{-3}
2c	BWR	54.1	1.02	166	85	10	600			0.4, 0.04, RH < 60 %	3×10^{-3}, 3×10^{-4}, RH < 60 %
3	BWR	68.78	1.25	166	85	5	600	N/A		0.4	3×10^{-3}
4	BWR	68.78	1.25	166	85	2	600	N/A		0.4	3×10^{-3}
5	BWR	68.78	1.25	166	85	1	600	N/A		0.4	3×10^{-3}
6	BWR	68.78	1.25	166	85	10	30	N/A		0.4	3×10^{-3}
7	BWR	68.78	1.25	166	85	5	30	N/A		0.4	3×10^{-3}
8	BWR	68.78	1.25	166	85	2	30	N/A		0.4	3×10^{-3}
9	BWR	68.78	1.25	166	85	1	30	N/A		0.4	3×10^{-3}
10	BWR	68.78	1.25	166	85	5	0	600	1.8	0.4	3×10^{-3}
10a	BWR	68.78	1.25	166	85	5	0	600	1.8	Zero for RH < 60 %	Zero for RH < 60 %
11	BWR	68.78	1.25	166	85	5	0	30	1.8	0.4	3×10^{-3}
11a	BWR	68.78	1.25	166	85	5	0	30	1.8	Zero for RH < 60 %	Zero for RH < 60 %
12	PWR	42.52	1.44	57	110	10	600	N/A		0.4	3×10^{-3}
13a	**PWR**	**42.52**	**1.44**	**238**	**110**	**10**	**600**	**N/A**		**0.4**	**3×10^{-3}**
13b	PWR	27.8	1.2	238	110	10	600	N/A		0.4	3×10^{-3}
13c	PWR	27.8	1.2	238	110	10	600	N/A		0.04	3×10^{-4}
13d	PWR	42.52	1.44	238	70	10	600	N/A		0.4	3×10^{-3}
13e	PWR	27.8	1.2	238	70	10	600	N/A		0.4	3×10^{-3}
13f	PWR	42.52	1.44	238	110	10	600	N/A		Zero for RH < 60 %	Zero for RH < 60 %
14	PWR	42.52	1.44	238	110	5	600	N/A		0.4	3×10^{-3}
15	PWR	42.52	1.44	238	110	2	600	N/A		0.4	3×10^{-3}
16	PWR	42.52	1.44	238	110	1	600	N/A		0.4	3×10^{-3}
17	PWR	42.52	1.44	238	110	10	30	N/A		0.4	3×10^{-3}
18	PWR	42.52	1.44	238	110	5	30	N/A		0.4	3×10^{-3}
19	PWR	42.52	1.44	238	110	2	30	N/A		0.4	3×10^{-3}
20	PWR	42.52	1.44	238	110	1	30	N/A		0.4	3×10^{-3}
21	PWR	42.52	1.44	238	110	5	0	600	1.8	0.4	3×10^{-3}
22	PWR	42.52	1.44	238	110	5	0	30	1.8	0.4	3×10^{-3}

* Temperature profile given in Figure 3-3 used and dose rate given by Equation 3-1.

3.2 KBS-3 BWR canister model results

Case 1 represents the BWR fuel canister conditions, for a low dose rate, while Cases 2–11 use a more conservative higher dose rate. Cases 2a–c examine the impact of changing geometry and corrosion rate, while Cases 3–5 investigate the effect of the amount of air impurity. Cases 6–9 also look at the impact of the amount of air but with lower initial water content. Cases 10 and 11 investigate the consequences of adding water gradually to the system as well as the effect of lowering the corrosion rate at low relative humidity (RH).

3.2.1 Cases 1 and 2a – Sensitivity to initial dose rate

Case 1 simulates the situation in which the water content of the canister is relatively high (12 failed fuel rods), there is significant (10 %) air trapped during backfill with Ar and corrosion is occurring on the iron surface. The initial dose rate is low though, 39 Gy/h compared to the equivalent base case results, Case 2a, in which the dose rate is 166 Gy/h.

Figures 3-4 and 3-5 show the canister temperature, pressure and dose rate output from the model for the first 500 years for Cases 1 and 2a.

The temperature and pressure dependence in Figures 3-4 and 3-5 are almost identical, but Figure 3-4 shows the expected lower initial dose rate. The initial increase in canister pressure is a consequence of the temperature rise and vaporisation of the liquid water present.

Figures 3-6 and 3-7 show the behaviour of oxygen, total water (liquid + gas), and corrosion rates for Cases 1 and 2a.

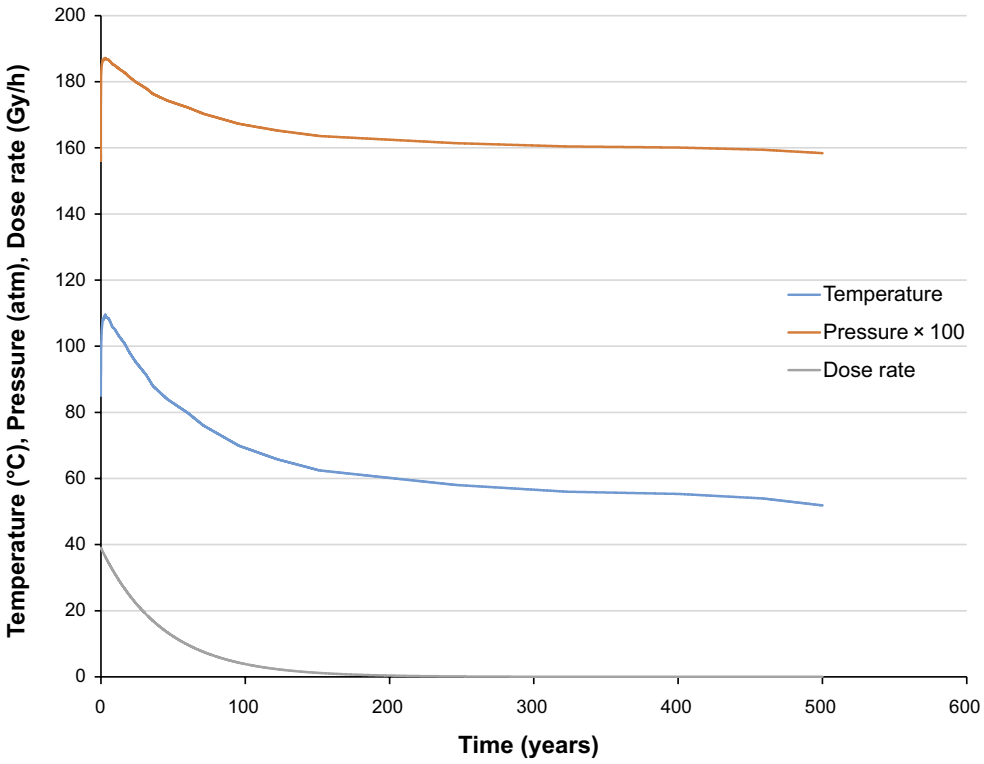

Figure 3-4. *Model calculated temperature, pressure and dose rate for Case 1.*

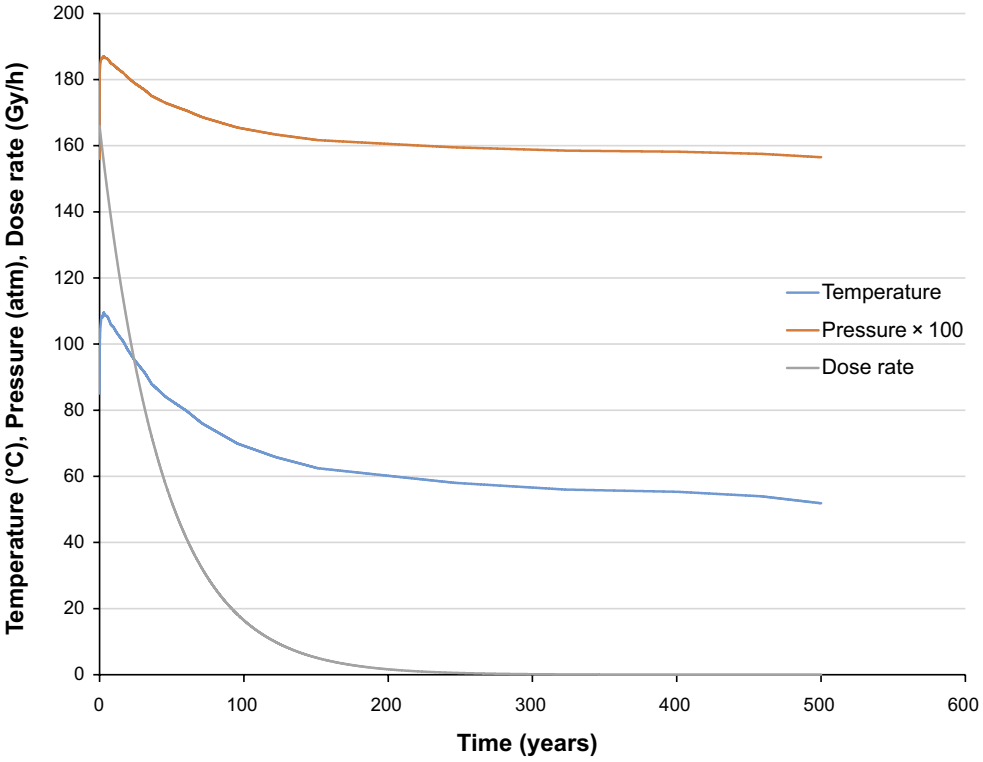

Figure 3-5. *Model calculated temperature, pressure and dose rate for Case 2a.*

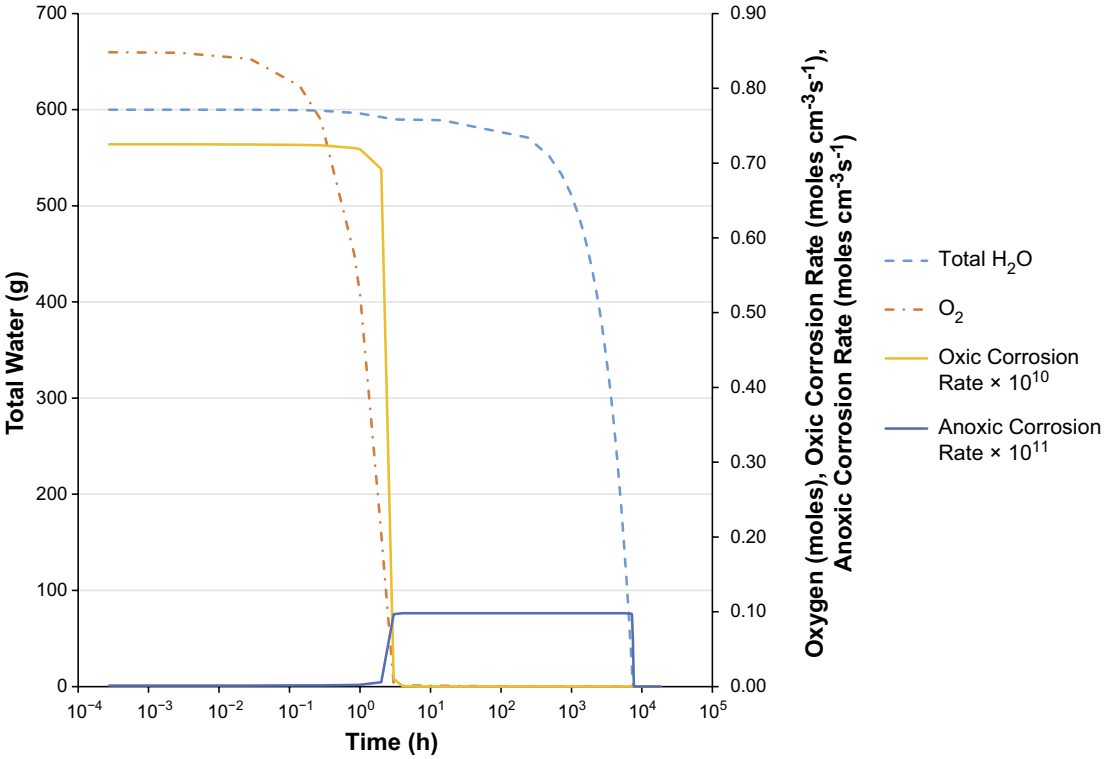

Figure 3-6. *Model outputs of canister water, oxygen, and corrosion rates versus time for Case 1.*

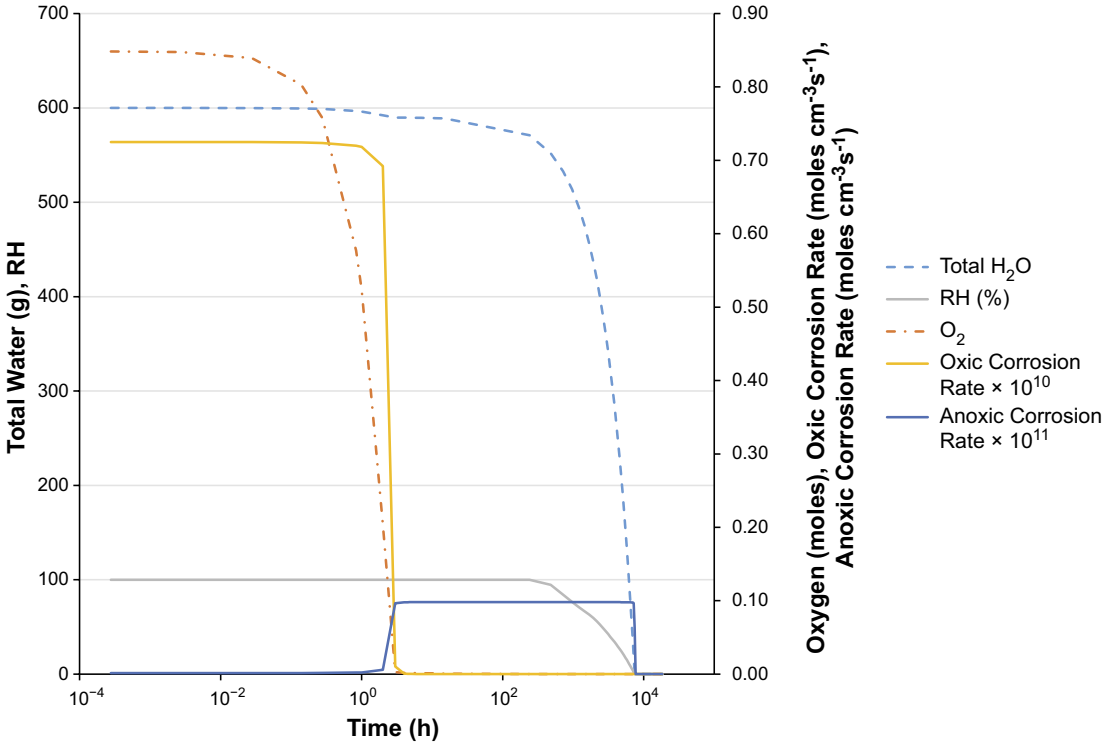

Figure 3-7. *Model outputs of canister water, oxygen, and corrosion rates versus time for Case 2a.*

The behaviour is almost identical for both cases. The figures show aerobic (Oxic) oxidation occurring until all the O_2 in the system is consumed, at which point anaerobic (Anoxic) corrosion takes over and carries on until all the water in the canister is consumed. Figure 3-7 also shows the relative humidity in the system, which starts to fall once there is no liquid water present, which is around 480 h (20 days), as can be seen in Figure 3-8 which shows the behaviour of the main stable species in the system for Case 1.

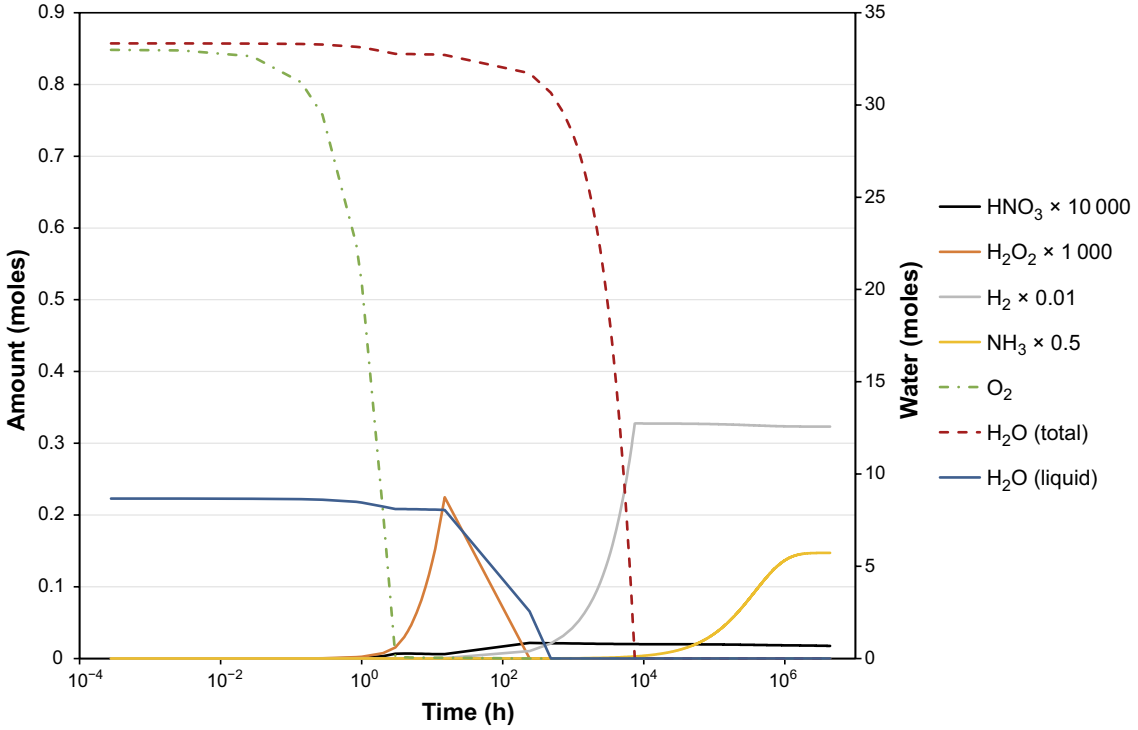

Figure 3-8. *Calculated major species amounts for Case 1, 600 g H_2O, 10 % air, corrosion, low dose rate (initially 39 Gy/h).*

Figure 3-9 is the equivalent figure to Figure 3-8 for Case 2a at the higher base case dose rate.

The relatively rapid loss of oxygen from corrosion for both theses cases means very little HNO_3 and H_2O_2 are produced. The sharp changes in species amounts observed on these plots are associated with sharp changes in conditions within the canister. For example, the sharp change in peroxide concentration is caused by the loss of O_2 (aerobic corrosion), the fall in liquid water content (anaerobic corrosion) and the production of significant amounts of gaseous H_2. The radiolysis chemistry indicates once H_2 reaches a threshold it tends to suppress peroxide formation. The two major species present in the system at the end of the calculation period are therefore NH_3 and H_2 and Figure 3-10 shows how the amounts of these species compare for the two cases.

The higher the dose rate the larger the amount of NH_3 produced. There is a corresponding drop in the final H_2 concentration as this is used in forming the additional NH_3 at the higher dose rate. It should be noted that at the end of the calculation there is excess H_2 in the system, roughly 30 moles, compared to the 0.2 (low dose rate) or 1.2 (high dose rate) moles of NH_3.[9] There is also excess N_2 in the system; the initial amount of N_2 present is approximately 3.3 moles. At approximately 100 years a quasi steady state is achieved where further slow changes are caused by decreasing dose rate and temperature. The final steady state amount of NH_3 formed is determined when its chemical formation and destruction mechanisms balance, which clearly depends on dose rate. For Cases 1 and 2a the initial dose rate increased by a factor of 4 from Case 1 to Case 2 and this resulted in a factor of 6 increase in the final ammonia concentration. From Figure 3-10 it is also clear that at the higher dose rate ammonia starts being produced in significant amounts sooner, at approximately 200 days, compared to 400 days at the low dose rate. From Figure 3-9, at the higher dose rate, there is water still present in the system, but no liquid water, when ammonia starts to form. At 200 days, for Case 2a, the relative humidity is only 24 % and in general the lower the relative humidity the less corrosion, see for example Samie et al. (2007). In some studies, however, corrosion rates have peaked at 45 % RH (Lapuerta 2008, iron corrosion), but these were under oxidising conditions. Whether 24 % RH in an Ar atmosphere containing NH_3 is corrosive is not known to the authors. In the remainder of this document the time when the RH falls below 60 % will be assumed to be the cut off point for a potential change in corrosion mechanism and therefore change in the corrosion rate.

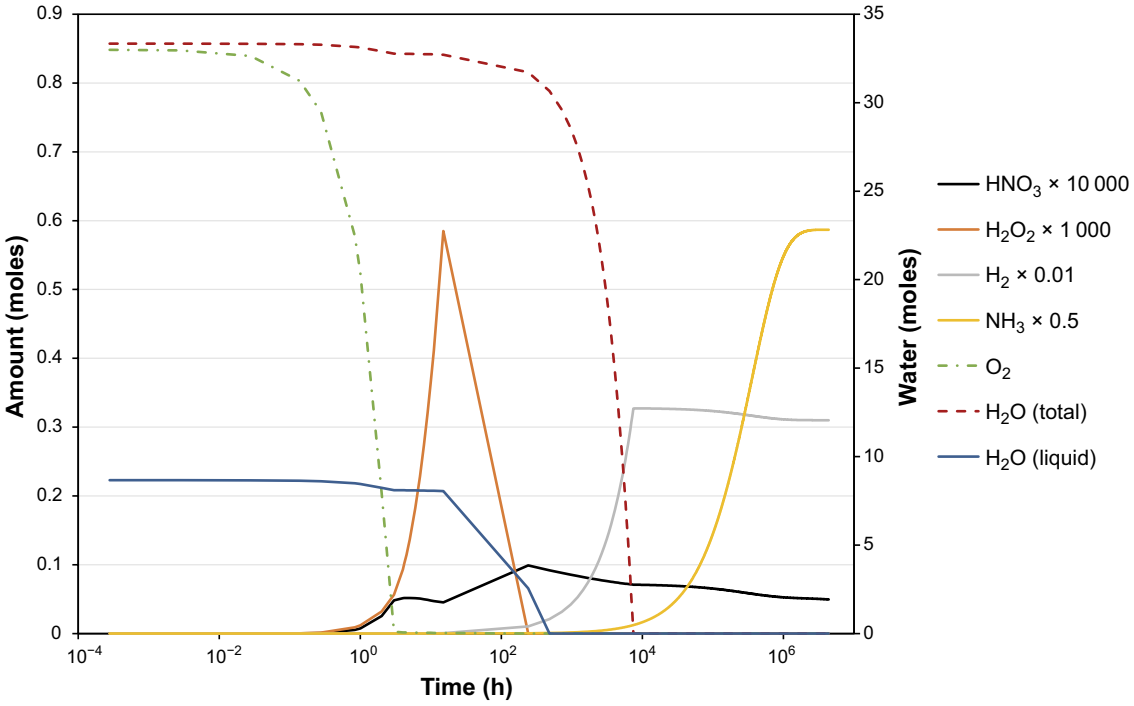

Figure 3-9. *Calculated major species amounts for Case 2a, 600 g H_2O, 10 % air, corrosion, base dose rate (initially 166 Gy/h).*

[9] Note 30 moles of H_2 in the final state corresponds to almost all the initial amount of water in the system (33.3 moles of H2) minus a) the amount occurring as the oxic corrosion product FeOOH, which, with 0.825 moles of O_2 would be around 0.55 moles of H_2, and b) the amount of H_2 in the NH_3 generated.

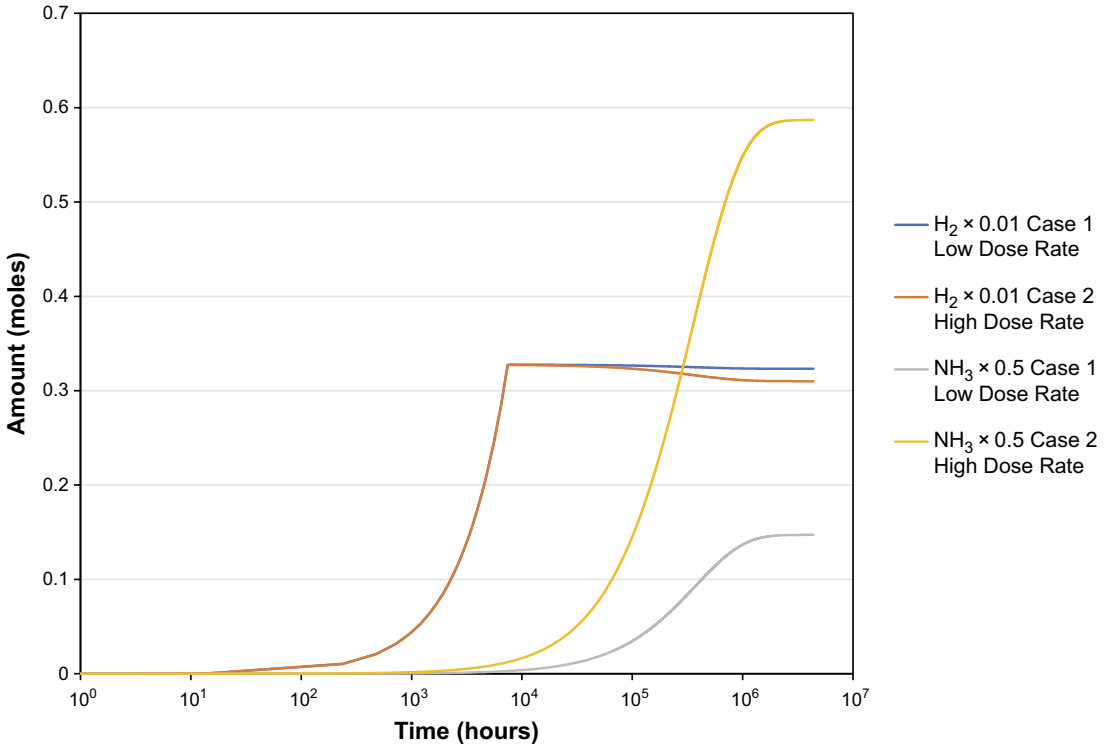

Figure 3-10. *Calculated NH_3 and H_2 amounts for Cases 1 and 2a.*

3.2.2 Case 2b – Sensitivity to steel area and system volume

As a base case, the steel area and system volume include the area and volume between the insert and the copper overpack, since it is assumed the gasket sealing the insert has failed. However, it may be that the gasket remains intact for the duration of the timeframe relevant for the processes investigated here. Therefore, Case 2b investigates the effects of smaller area and volume. From Table 3-1 Case 2b differs from 2a in that the steel surface area and gas volume in the system have been reduced by approximately 20 %. Figure 3-11 shows the variation in temperature, pressure and dose rate for Case 2b.

Comparing with the equivalent figure for 2a, Figure 3-5, indicates a higher pressure is achieved here, reflecting the reduction in the system volume. Since some of the chemical rate constants in the model have a pressure dependence (see Henshaw and Spahiu 2021) this will impact the chemistry. Figure 3-12 is a plot of the corrosion rates along with O_2 gas and total H_2O behaviour for Case 2b. Also plotted is the O_2 and total H_2O for Case 2a.

Case 2b has a smaller system volume than Case 2a and so the total amount of O_2 initially present is smaller. However, the lower system area for 2b means a slower removal rate of O_2 by corrosion. The overall net impact on the O_2 removal time by corrosion from changing these system variables is small. In the case of H_2O the smaller system area for 2b compared to 2a means it takes longer to remove all the water from the system, 9 600 h (400 days) compared to 7 440 h (310 days) for 2a.

Figure 3-13 shows the ammonia and hydrogen behaviour for Case 2b, along with the equivalent plots for Case 2a. Also shown on the Figure is the behaviour of water for Cases 2b and 2a. Reducing the system area and volume has led to a decrease in the steady state amount of ammonia produced. This is most likely a consequence of the reduced volume meaning less N_2 initially present in the system (there are also changes in chemical reaction rates including changes in some of the pressure dependent rate constants). Figure 3-13 also shows though that liquid water and RH remain high for a longer period for Case 2b, and the period of time in which water and significant NH_3 co-exist in the system is longer for Case 2b.

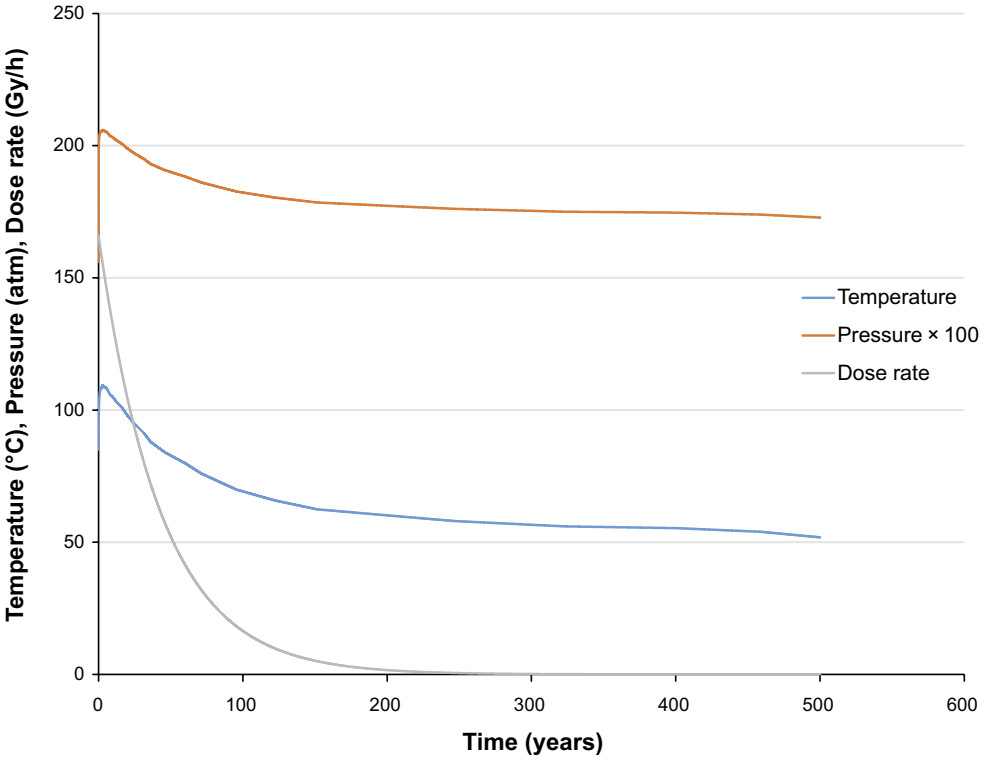

Figure 3-11. *Model calculated temperature, pressure and dose rate for Case 2b.*

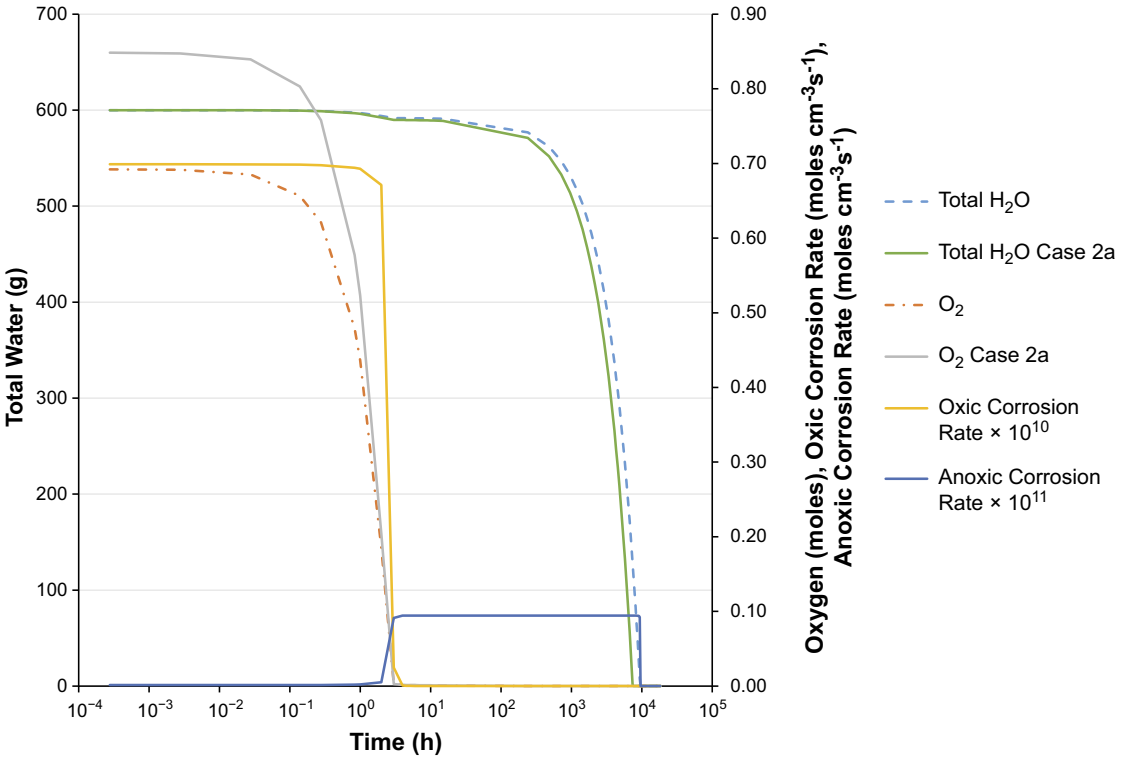

Figure 3-12. *Model outputs of canister water, oxygen, and corrosion rates versus time for Case 2b. Also plotted are the O_2 and total H_2O for Case 2a.*

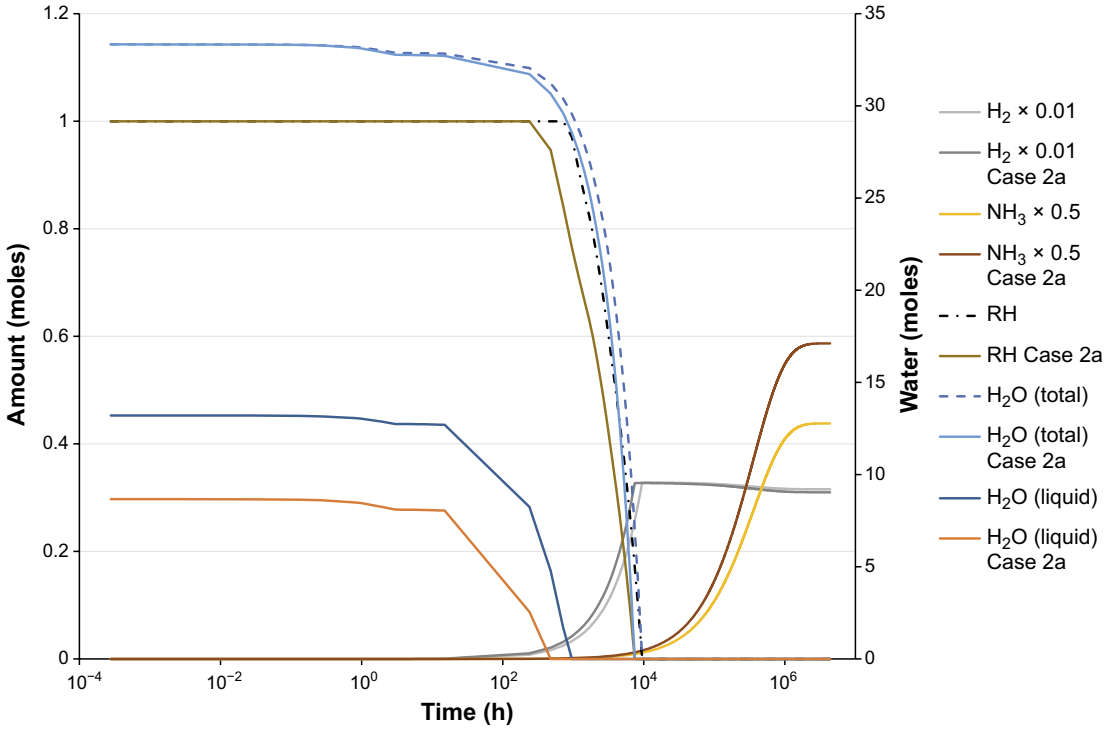

Figure 3-13. *Model outputs of canister NH_3, H_2 and water+RH for Case 2b. Also plotted are the equivalent model results for Case 2a (higher surface area and system volume).*

3.2.3 Cases 2c – Sensitivity to system corrosion rate

For Case 2c the model was set up with the same steel area and system volume as for Case 2b, but the aerobic and anaerobic corrosion rates were reduced by a factor of 10 once the relative humidity fell below 60 %. From Figures 3-12 and 3-13 it is clear that oxygen in the system will have been removed by corrosion before RH falls below 60 %, so this modification will have no effect on aerobic corrosion, but it may impact the result of anaerobic corrosion. Figure 3-14 is a plot of the corrosion rate and relative humidity calculated by the model as a function of time, the fall in anaerobic corrosion rate is visible at a RH of 60 %. Figure 3-15 shows the major species amounts versus time, also on this figure is a plot of NH_3 from Case 2b, identical initial conditions as for 2c but with no change in corrosion rate. The change in corrosion rate impacts the rate of production of H_2, but there is excess H_2 at this point in the development of the gas composition and it has little effect on the predicted NH_3 results, compared to the results for Case 2b.

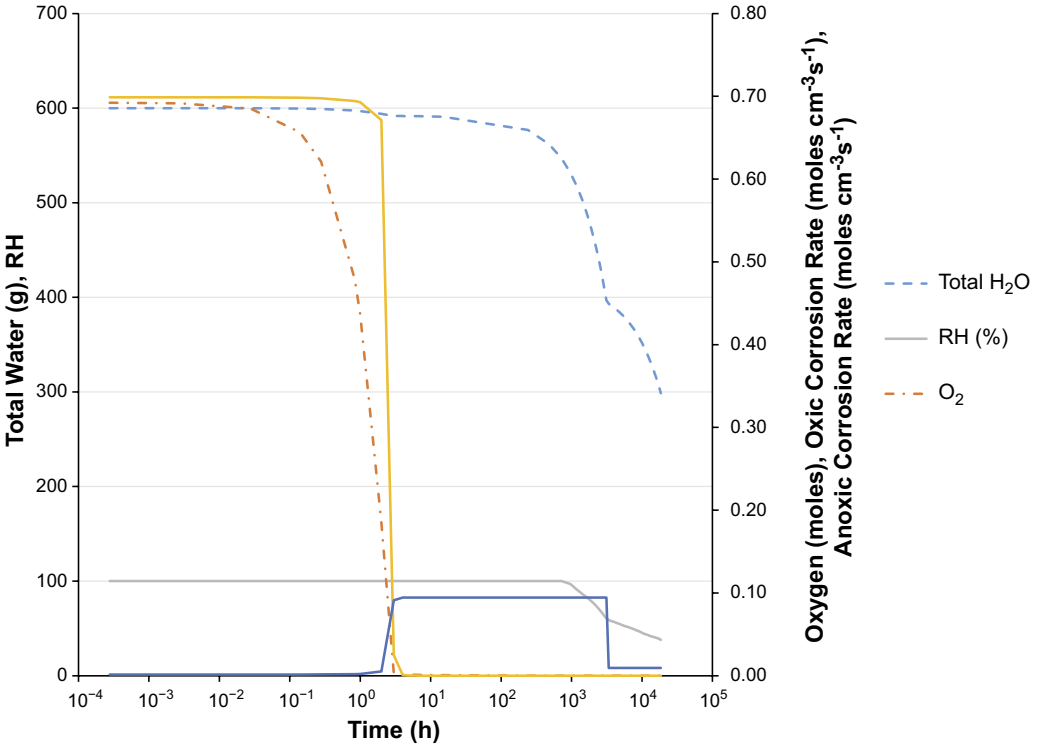

Figure 3-14. *Model outputs of canister water, oxygen, and corrosion rates versus time for Case 2c.*

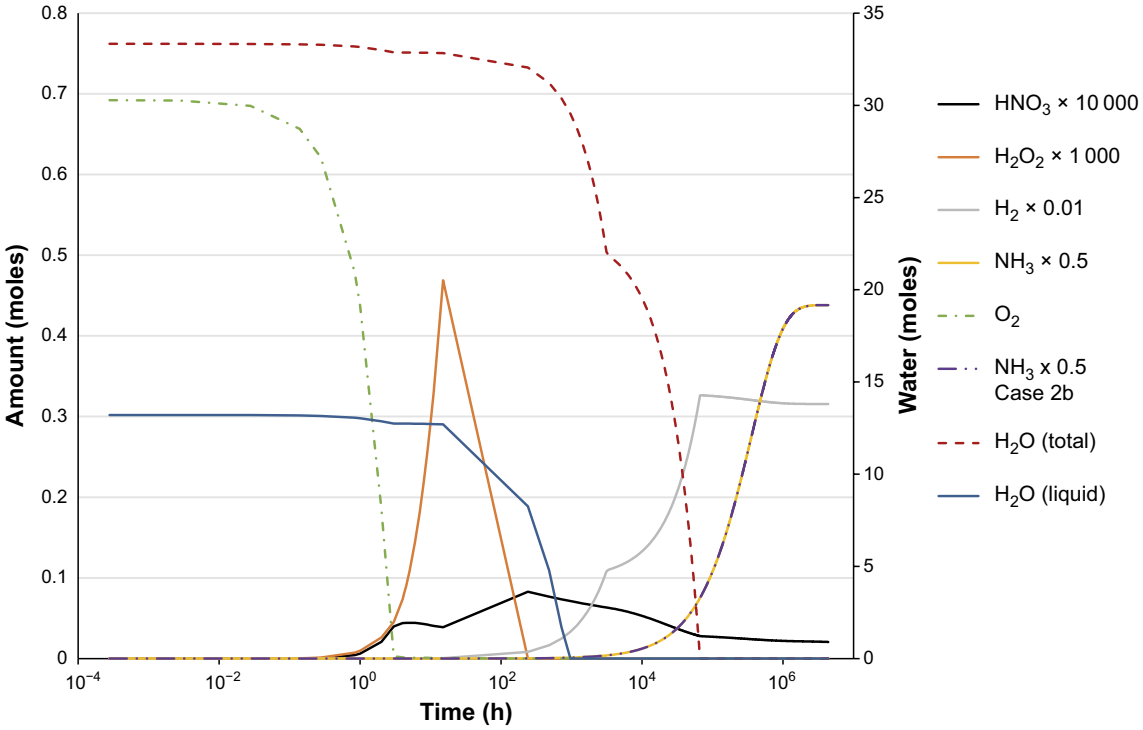

Figure 3-15. *Calculated major species amounts for Case 2c. Also plotted NH_3 concentration from Case 2b, results overlap Case 2c.*

3.2.4 Case 6 – Impact of reducing initial water content

Case 6 considers the same conditions as Case 2a, but with 30 g of water initially present instead of 600 g. Figure 3-16 shows the main stable species amounts versus time for Case 6. There is no liquid water for these conditions.

Comparing Figure 3-16 (Case 6, 30 g water) with Figure 3-9 (Case 2a, 600 g water) indicates a significantly lower production of the major species H_2 and NH_3 at the lower water content. This is emphasised in Table 3-2 which tabulates the peak amounts of each species for Cases 2a and 6.

Table 3-2. Peak amounts of main species for Cases 6 and 2a.

Species	Case 2a Peak Amount (moles)	Case 6 Peak Amount (moles)
H_2	32.7	1.1
NH_3	1.25	0.735
H_2O_2	5.8×10^{-4}	2.6×10^{-4}
HNO_3	9.9×10^{-6}	1.2×10^{-5}

There is a small increase in the amount of nitric acid (of which there is very little) probably a result of the slightly more oxidising conditions (less H_2 in the system). It should be noted though that although the water content has been reduced by a factor of 20 the amount of ammonia at steady state has only reduced by a factor of 1.7. This is partly a consequence of the assumption that the same dose rate applies to both Cases 2a and 6 and how this dose rate is partitioned amongst the various species in the gas, which is discussed further in the following section.

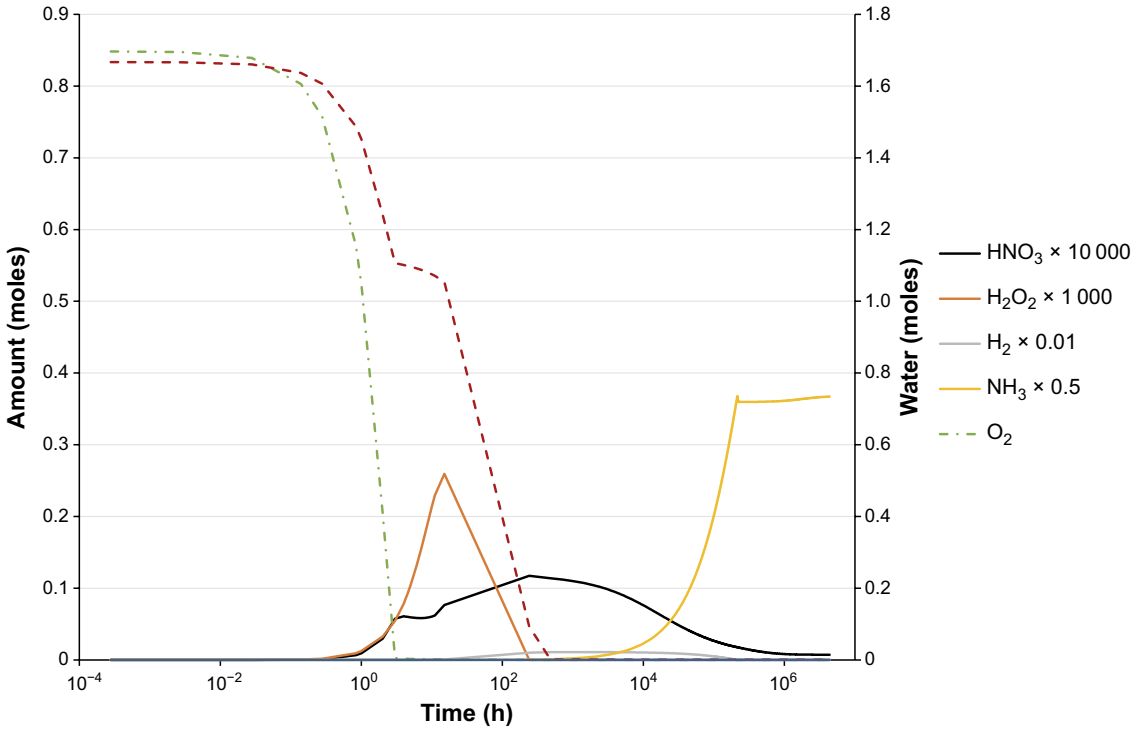

Figure 3-16. *Calculated major species amounts for Case 6.*

3.2.5 Cases 2a, 3, 4, 5 and Cases 6, 7, 8 and 9 – Impact of initial air content

For Cases 2, 3, 4, 5 the initial water in the canister was 600 g but the amount of air present was decreased, 10 %, 5 %, 2 % and 1 %. Cases 6, 7, 8 and 9 are at the same air contents respectively but for 30 g of water in the system. Figure 3-17 is a plot of the steady state amount of ammonia predicted by the model for these 8 cases versus the initial amount of air in the canister.

Figure 3-17 generally indicates the more air present in the canister the greater the amount of ammonia formed. In simple terms H_2 generated from H_2O in the system reacts with N_2 to form NH_3 and the more N_2 present the greater the amount of NH_3. This simple picture would suggest for the 10 % air case compared to the 5 % air there should be more NH_3. This is clearly what is happening in the 600 g water cases but not in the 30 g water cases. The fall in the amount of NH_3 produced at 10 % air and 30 g H_2O is related to corrosion processes occurring in the system, which have already been discussed but are repeated here (Equations 3-2 and 3-3):

Aerobic corrosion: $4Fe + 2H_2O + 3O_2 = 4FeOOH$ (3-2)

and

Anaerobic corrosion: $3Fe + 4H_2O = Fe_3O_4 + 4H_2$ (3-3)

The aerobic reaction (Equation 3-2) is much faster and occurs until all the O_2 is consumed, at which point the anaerobic corrosion process (Equation 3-3) becomes the dominant reaction. Aerobic corrosion consumes H_2 previously bound up in H_2O, forming FeOOH, while anaerobic corrosion releases H_2 (previously bound in H_2O). The more O_2 present the more H_2 is removed by aerobic corrosion, so the 10 % air case will consume more H_2 via aerobic corrosion than the 5 % air case. This means there is less H_2 available to form NH_3 and why the amount of ammonia formed in the 10 % air and 30 g case is less than case for 5 % air. In the cases for 600 g of water this doesn't happen because there is so much excess H_2 around from water, compared to the levels of N_2 and O_2, that the loss of a small amount of H_2 to corrosion is not important. Likewise, when the air amount is low, 1 or 2 %, and therefore the amount of O_2 is low, the amount of H_2 lost through aerobic corrosion is not important. It's easy to see what's happening by examining Figure 3-18 which shows on the y-axis the number of moles of H_2, originally present as H_2O, that has formed FeOOH (corrosion) or NH_3, for the cases with 5 % and 10 % air with 30 g of water present. 30 g of water amounts to 1.67 moles of H_2 and from Figure 3-18, at 5 % air, roughly 0.3 moles of the H_2 is consumed in the corrosion process, leaving 1.37 moles to form NH_3. At 10 % air 0.6 moles of H_2 is consumed by aerobic corrosion, leaving only 1.07 moles to form ammonia, hence less ammonia is formed in the 10 % air case.

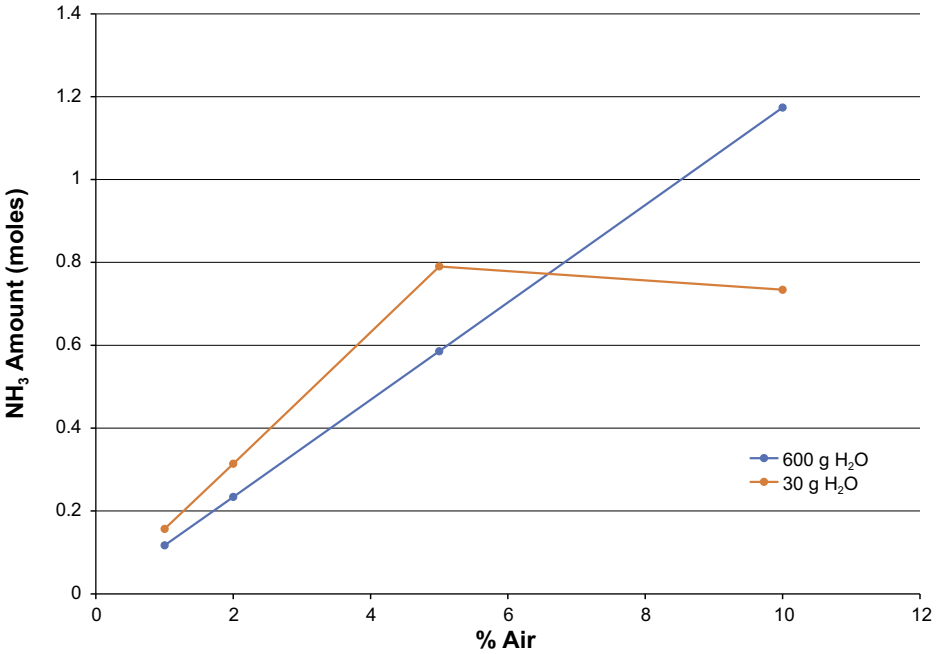

Figure 3-17. *Calculated final amounts of NH_3 for Cases 2a, 3, 4, 5, 6, 7, 8, 9 against initial air content of the canister.*

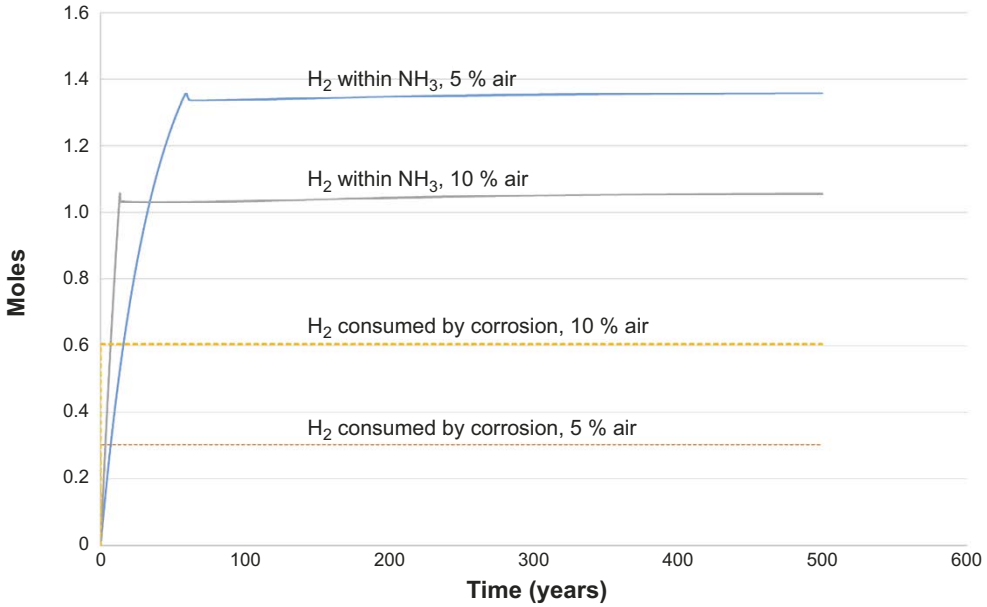

Figure 3-18. *Plot of H_2 consumed by aerobic corrosion and converted to NH_3, for Cases 6 (10 % Air/30 g H_2O) and 7 (5 % Air/30 g H_2O).*

Of course, starting with 600 g of water, i.e. 33.3 moles of H_2, removing 0.3 moles or 0.6 moles of H_2 by aerobic corrosion would not be important as there is still over 30 moles of H_2 available to react with all the N_2 present (~3.7 moles for 10 % air and 1.85 moles for 5 % air).

Figure 3-17 also indicates at low % air content more NH_3 is formed in the 30 g of H_2O than in 600 g of H_2O. The model assumes the same dose rate for all cases, which is partitioned amongst the gas constituents roughly in proportion to their molar fraction in the gas.[10] There is approximately 40 moles of Ar in the gas space, for 5 % air approximately 2 moles of N_2 and for 600 g H_2O (if all in the gas phase) approximately 30 moles, for 30 g H_2O approximately 2 moles. Most of the dose rate is therefore partitioned into Ar, the largest constituent of the gas, but at high water content a significant fraction goes into H_2O with only a small fraction to N_2. At low water content, however, the fraction of radiation affecting N_2 and H_2O is similar and the dose rate to N_2 will be larger than in the 600 g water case. This change in partitioning of the dose rate amongst the various species means essentially there will be more primary interactions of the radiation with N_2 at low water content leading to the formation of the N atom from these initial interactions. This primary interaction of the radiation with N_2 is probably the most important process in determining the amount of NH_3 that is formed, which is why at low water content more NH_3 is formed provided there is adequate supply of hydrogen. As stated above though, at high air content and low water the supply of H_2 limits the amount of ammonia that can be formed.

3.2.6 Cases10 and 11 – Slow addition of water to the system

The conditions for Case 10 are nominally the same as for Case 3, except the 600 g of water present in the canister is released from the fuel pins slowly at a rate of 1.8 g/day. Note that this rate is based on estimates of the number of failed rods and the expected temperature evolution (see Section 3.1), so is highly uncertain. Note also that the maximum amount of water, 600 g, used in these calculations is not directly connected to the assumed number of failed rods. Figure 3-19 shows the behaviour of O2, water and both corrosion rates for Case 10. The calculation assumed 1 g of water was present in the system at the start of the calculation. The plot shows that the 600 g of water are added after 8 000 h and no further H_2O is added to the system, but the total water present never gets above 4 g as H_2O is consumed by corrosion. This is primarily anaerobic corrosion as O_2 is consumed by aerobic corrosion within the first 10 h. Therefore, compared with Case 3, in which the initial amount of water present was 600 g, much less water is experienced in the vapour phase here. When water addition to the system

[10] It also accounts for electron density but these are similar for the various species.

stops at 600/1.8 = 333.33 days (8 000 h) the water in the system is rapidly consumed and anaerobic corrosion stops. It should be noted that no mass transfer limitations nor changes in corrosion mechanism are assumed with respect to the corrosion rate, so at low water vapour pressure it is assumed water can arrive at the metal surface fast enough to maintain the assumed corrosion rate.

Figure 3-20 is a plot of the species amounts versus time for Case 10.

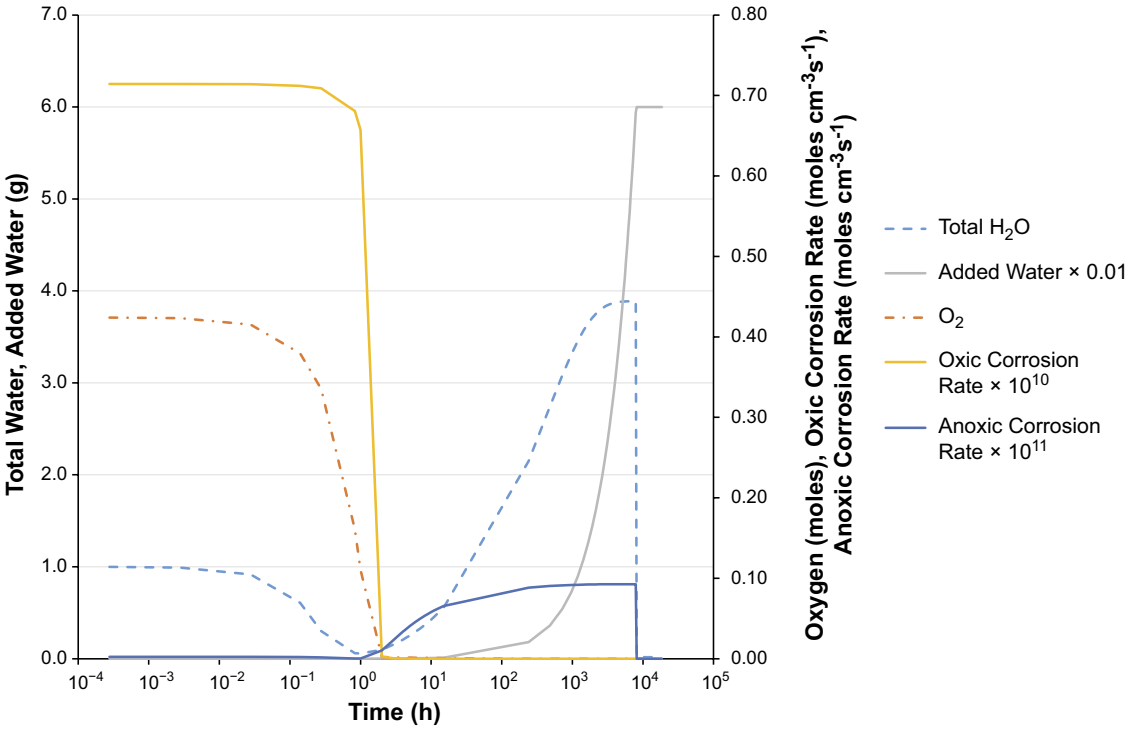

Figure 3-19. *Plot of O_2, total H_2O present, total added H_2O, and rates of aerobic and anaerobic corrosion for Case 10.*

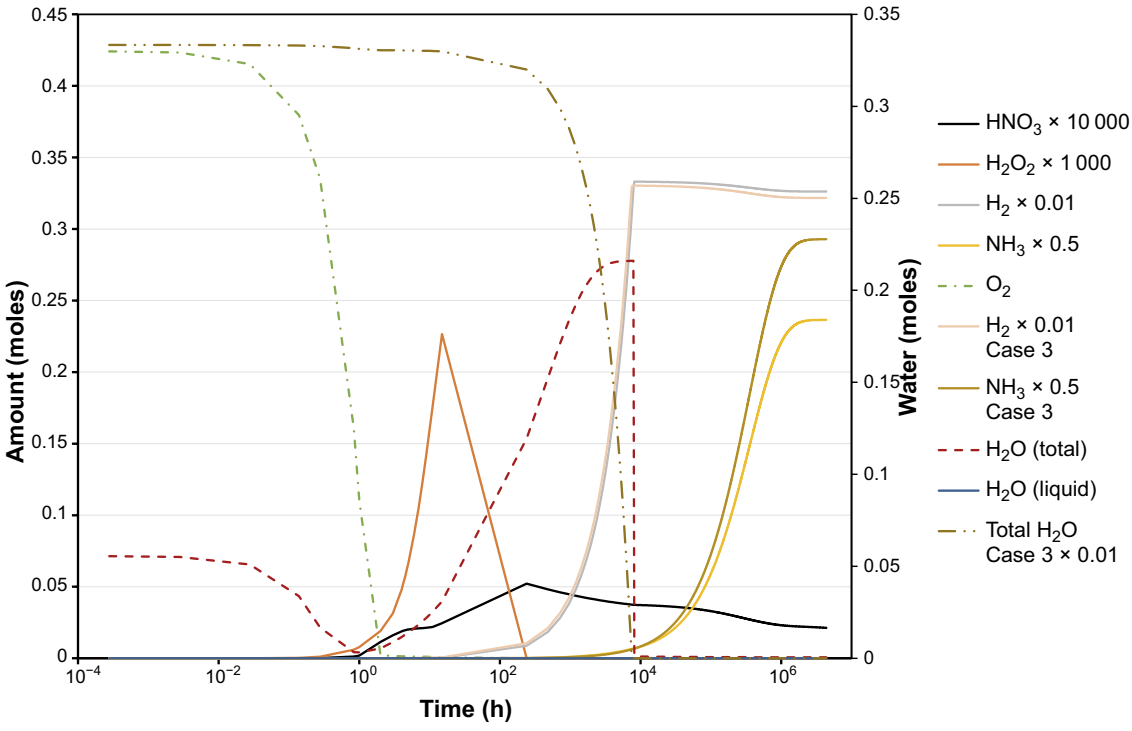

Figure 3-20. *Plot of species amounts versus time for Case 10. Also plotted is the NH_3 and H_2 behaviour for Case 3.*

Also plotted in Figure 3-20 are the NH_3. H_2 amounts and total water from Case 3, in which 600 g of H_2O was present at the start. Note the amount liquid water in Case 10 is zero. Figure 3-20 indicates adding the 600 g of water gradually leads to less conversion of H_2 and N_2 to ammonia, likely a consequence of lower amount of energetic species associated with water (e.g. radicals such as OH) at any point in time. The results indicate water and ammonia co-exist in the system for roughly the same period for Cases 3 and 10.

Figure 3-21 shows the behaviour of O_2, water and both corrosion rates for Case 11, also shown is the amount of H_2O that has been added to the system at a rate of 1.8 g/day.

The total water in the system rises to just above 2 g as H_2O is added and consumed by corrosion. When 30 g of water have been added, at 30/1.8 = 16.7 days (400 h), addition ceases and the amount of water in the vapour rapidly drops to zero as it is consumed by anaerobic corrosion. Figure 3-22 shows the behaviour of the main species in the gas phase with time for Case 11, also shown are the H_2, NH_3 and total amount of H_2O from Case 7, in which 30 g of water was present at the start (nominally all other initial conditions are identical to Case 11). Case 11 produces less NH_3 than in Case 7, but the difference is small and the temporal behaviour is similar. In both Case 7 and Case 11 at low water content water is consumed by corrosion before significant ammonia is formed.

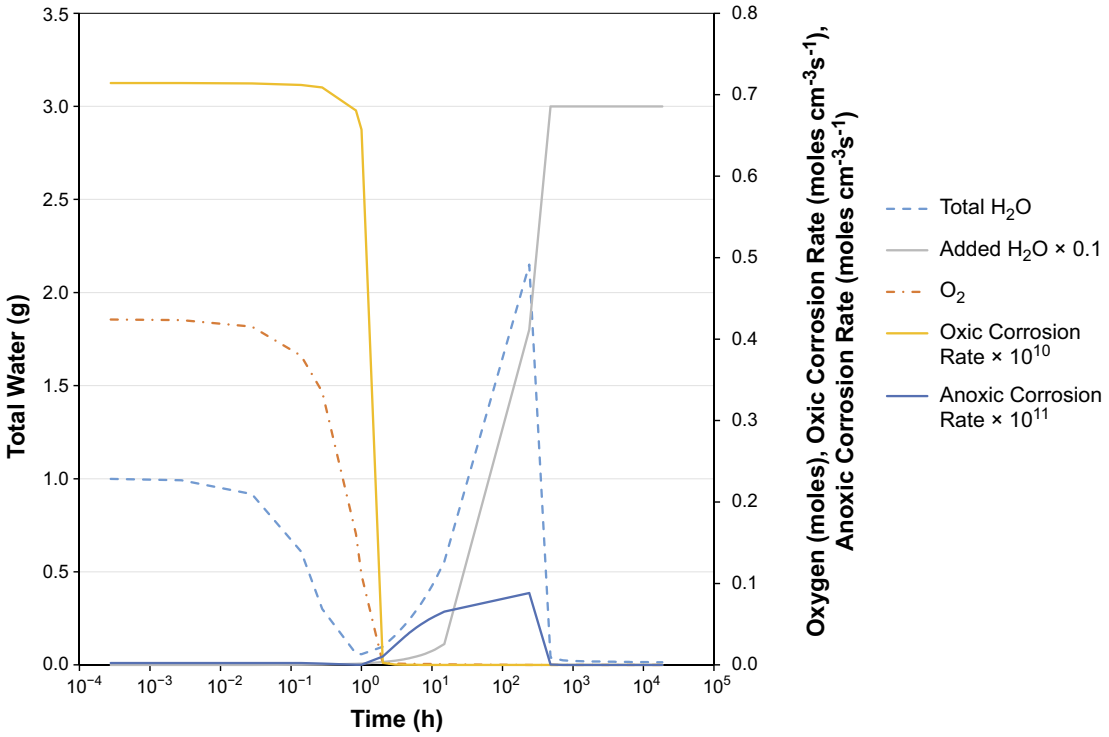

Figure 3-21. *Plot of O_2, total H_2O present, total added H_2O, and rates of aerobic and anaerobic corrosion for Case 11.*

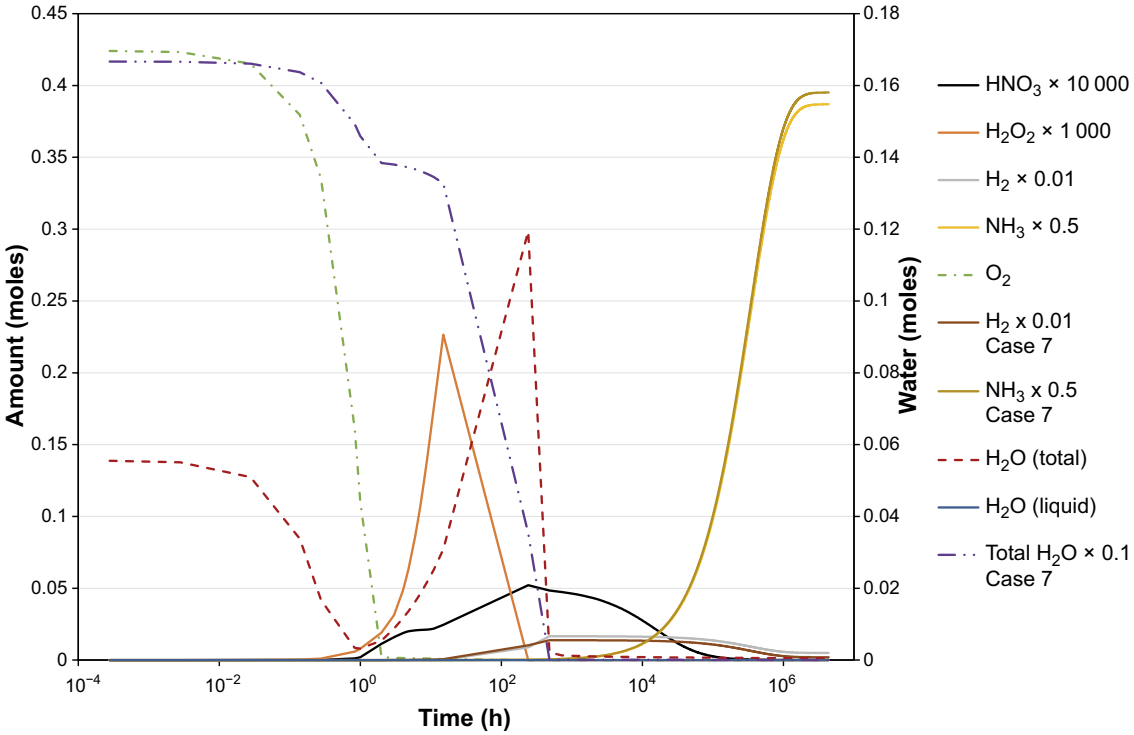

Figure 3-22. *Plot of species amounts versus time for Case 11. Also plotted is the NH_3 and H_2 behaviour for Case 7.*

3.3 KBS-3 PWR canister model results

3.3.1 Cases 12 and 13a – Sensitivity to initial dose rate

Figure 3-3 which shows the temperature behaviour in the KBS-3 canister indicates for PWR fuel this remains above 100 °C for the first ten years after encapsulation. A significant larger fraction of the water in the system therefore will be present in the vapour phase, compared to the BWR cases discussed previously. Figure 3-23 shows the model predictions of temperature, pressure and dose rate for Case 12. Figure 3-24 shows the predicted species amounts for Case 12. Water remains in the vapour phase throughout the simulation and comparing the H_2 and NH_3 levels with the analogous BWR Case 1 (Figure 3-8) indicates the predicted H_2 levels are similar but the NH_3 amount is significantly larger (0.5 moles for Case 12 compared to 0.3 moles for Case 1). RH is also plotted on Figure 3-24 and starts at approximately 0.51 (as a fraction) and decreases as water is consumed by radiolysis and corrosion. At the starting temperature for the PWR case roughly 1 200 g of water is required to saturate the gas phase.

Figure 3-25 plots the temperature, pressure and dose rate for Case 13a, showing the higher initial dose rate for this case compared to Case 12. Figure 3-26 shows the corresponding species amounts against time for Case 13a, identical to Case 12 except for this higher dose rate. Comparing Figures 3-24 and 3-26, increasing the initial dose rate from 57 to 238 Gy/h has increased the final steady state ammonia from approximately 0.5 moles to 1.9 moles and it has also increased the period of time water and NH_3 co-exist in the system. Comparing with Case 2a, the analogous BWR case, the amount of ammonia produced is again greater for Case 13a. The smaller surface area in the PWR case also mean water remains present in the system longer (Case 13a, 480 days) compared to the BWR cases (Case 2a, 310 days).

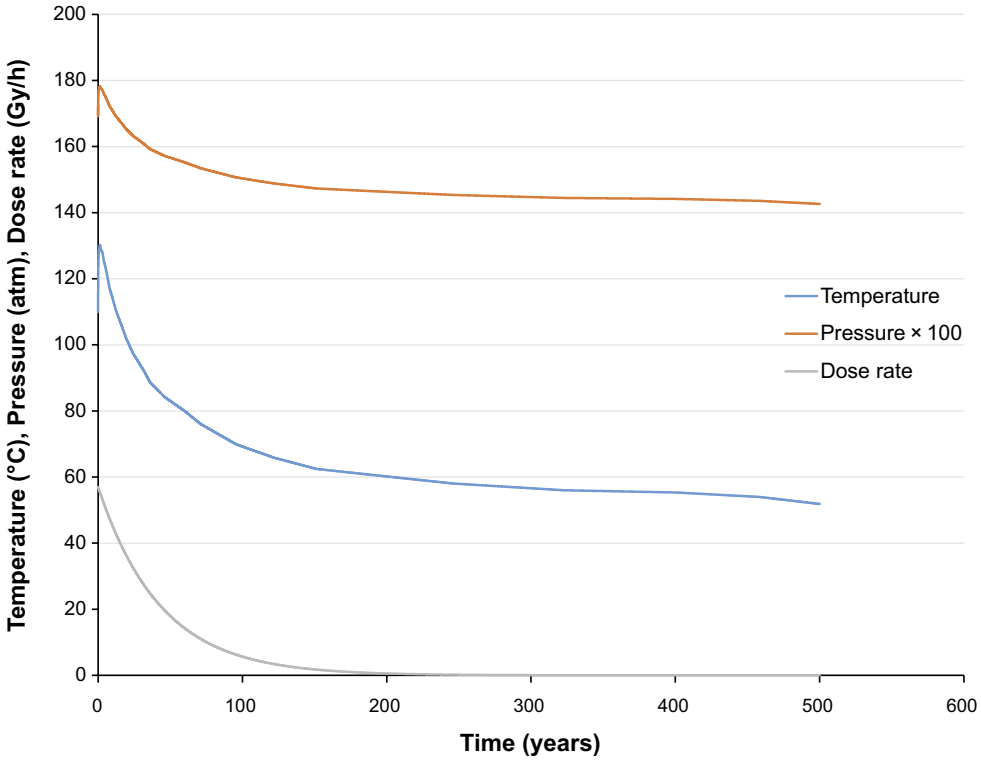

Figure 3-23. *Model calculated temperature, pressure and dose rate for Case 12.*

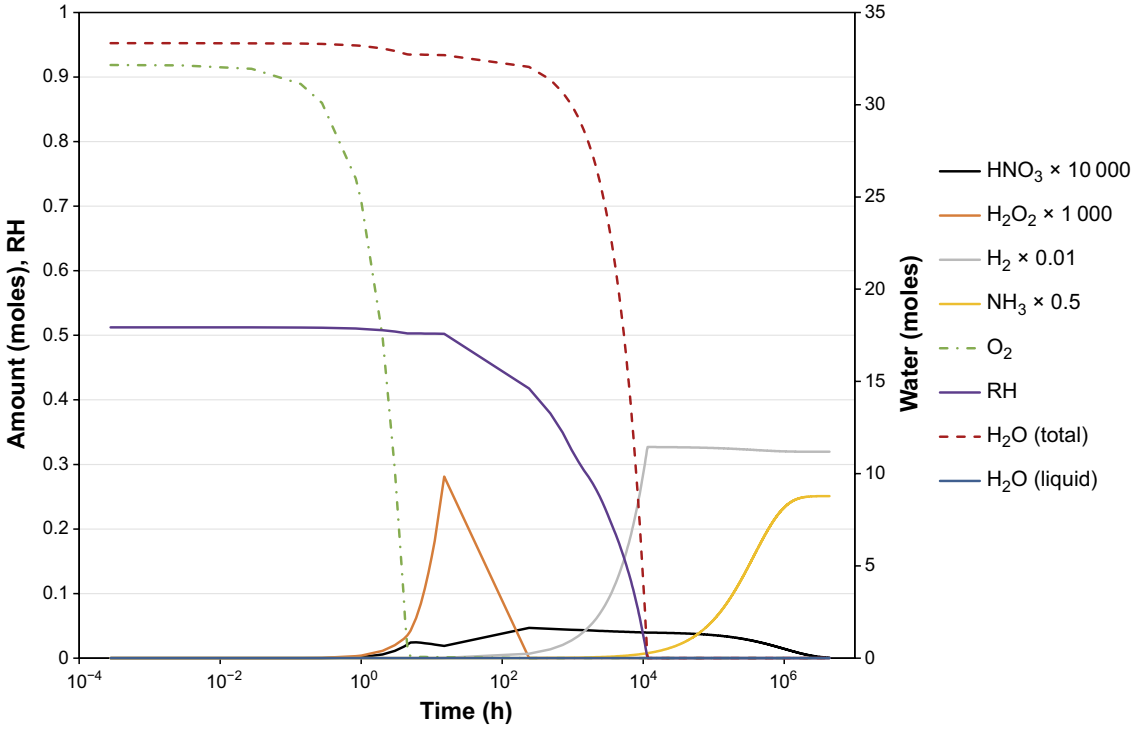

Figure 3-24. *Plot of species amounts, (also RH as fraction), versus time for Case 12. There is no liquid water in this case.*

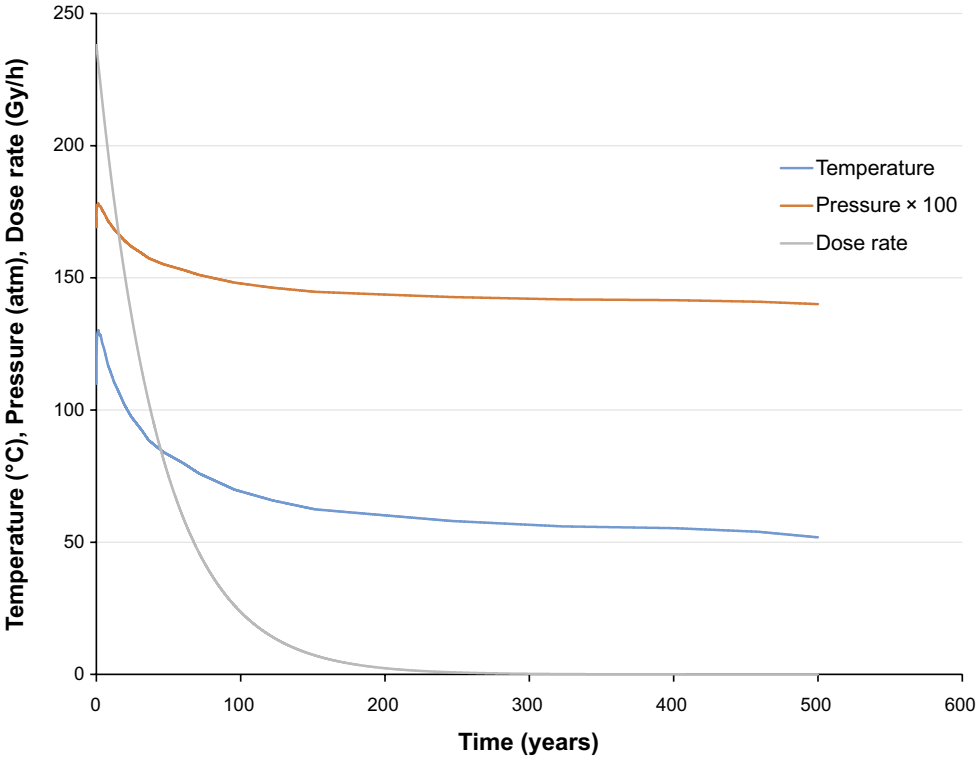

Figure 3-25. *Model calculated temperature, pressure and dose rate for Case 13a.*

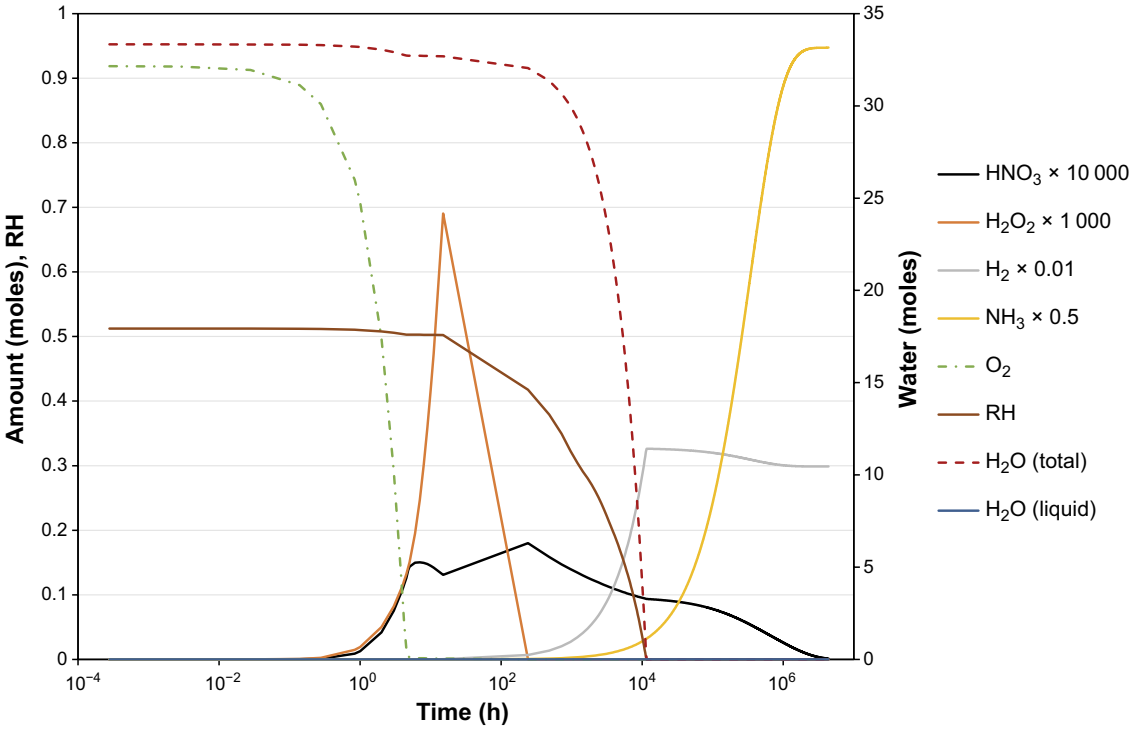

Figure 3-26. *Plot of species amounts versus time for Case 13a. There is no liquid water in this case.*

3.3.2 Case 13b – Sensitivity to initial steel area and system volume

Figure 3-27 is a plot of the amounts of H_2, NH_3 and total water for Case 13b. Case 13b used a smaller steel surface area and canister volume than the equivalent 13a case, the results of which are also shown in the Figure.

Decreasing the area available for corrosion from 1.44 m^2 to 1.2 m^2 increased the length of time water is present in the system from 510 to 760 days, ammonia starts become significant at around 50–60 days in both cases.

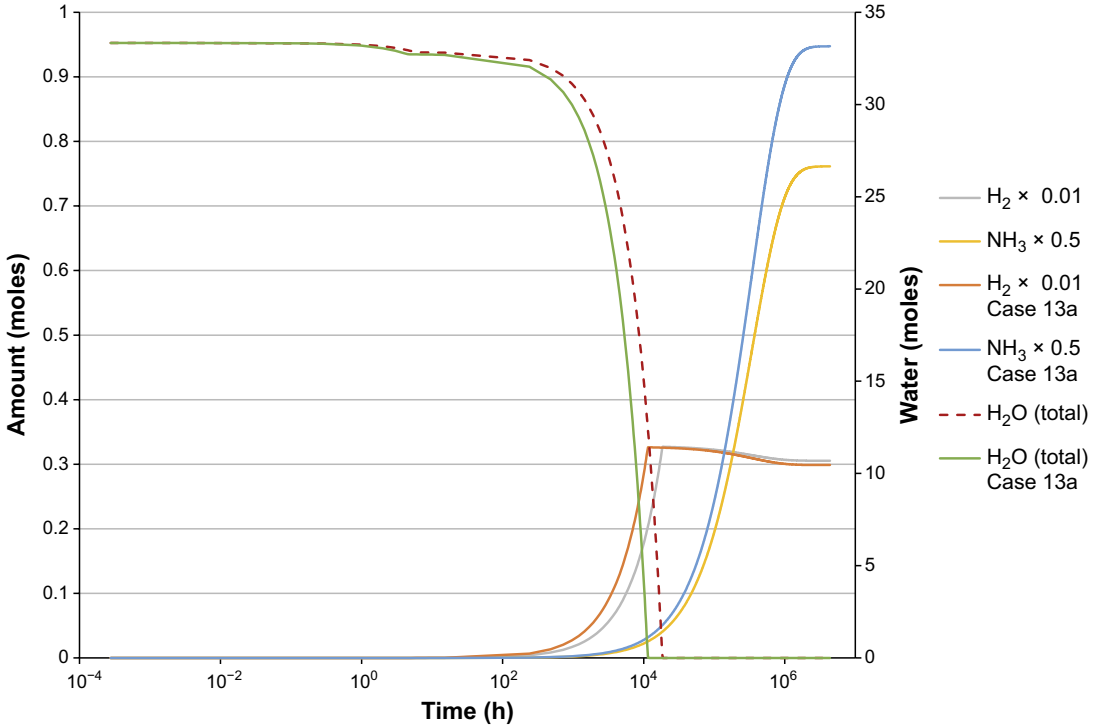

Figure 3-27. *Plot of H_2, NH_3 and total H_2O amounts versus time for Case 13b and Case 13a.*

3.3.3 Case 13c – Sensitivity to system corrosion rate

Case 13c is analogous to Case 13b except the corrosion rates have been reduced by a factor of 10. Figure 3-28 compares the results from Cases 13c and 13b. From this figure the time at which both O_2 and H_2O are removed from the system have increased as a consequence of the slower corrosion rate, in the case of O_2 from 7 to 240 h and for H_2O from 760 days to 7 600 days. The final steady state amounts of H_2 and NH_3 in the system, or their temporal behaviour, though have not changed significantly between Cases 13c and 13b.

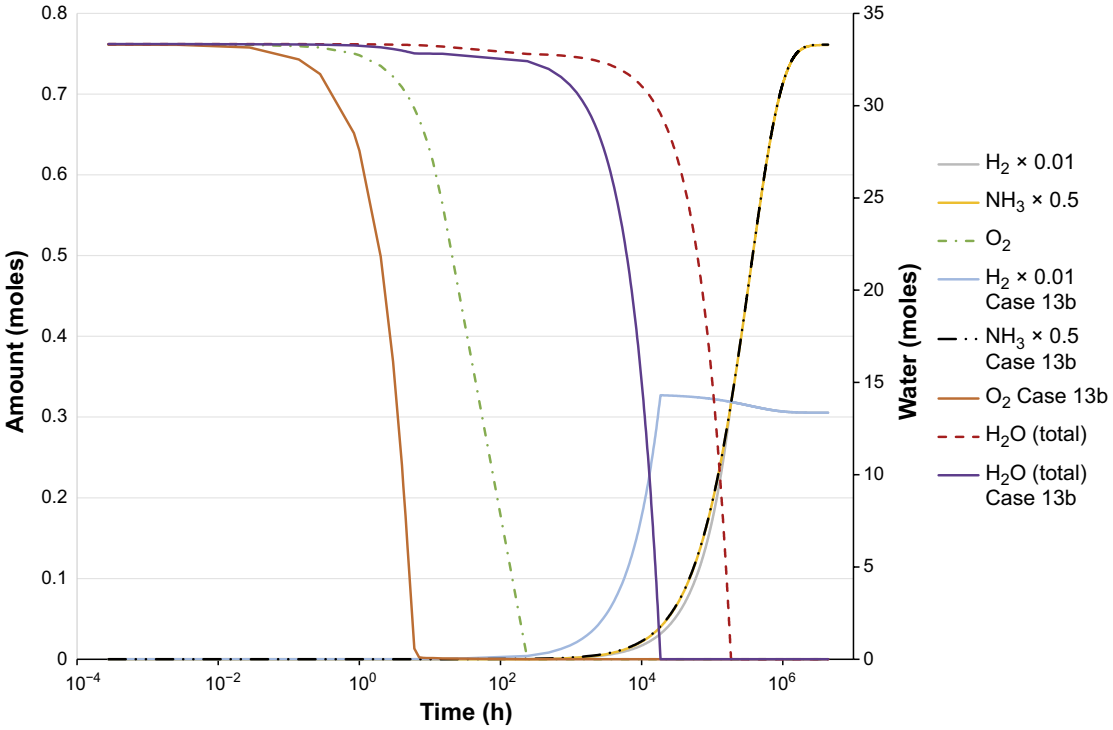

Figure 3-28. *Plot of H_2, NH_3 and total H_2O amounts versus time for Case 13c and Case 13b.*

3.3.4 Cases 13d and 13e – Sensitivity to initial system temperature

The standard PWR canister conditions discussed in Section 3.1 indicate that for PWR fuel the initial starting temperature is approximately 110 °C, a consequence of which is that H_2O is primarily in the vapour phase and therefore gaseous water amounts are high at the start and remain so until water is consumed by anaerobic corrosion. To investigate the impact of this high temperature, calculations for Cases 13e and 13d used a lower temperature profile for the PWR dose rates, at the high system volume/area and at the low system volume/area. The temperature profile used for these two cases is shown in Figure 3-29, which shows the temperature starting at 70 °C and reaching a maximum of 100 °C after several years of operation.

Figure 3-30 shows the species quantities for Case 13e versus time, along with the amounts of H_2O (liquid), H_2O (total), NH_3 and H_2 for Case 13a, the equivalent high temperature conditions. It is clear for Case 13e liquid water is present in the system for approximately 60 days, but compared to Case 13a were there is no liquid water present, this has little effect on the amounts of H_2 and NH_3 produced or the temporal behaviour of these species.

Figure 3-31 shows the species quantities for Case 13d versus time, along with the amounts of H_2O (liquid), H_2O (total), NH_3 and H_2 for Case 13b, the equivalent high temperature conditions. It is clear for Case 13d liquid water is present in the system for approximately 60 days. This has a small effect on the amount of NH_3 produced at steady state (falling from 1.52 moles for Case 13b to 1.48 moles for Case 13d) but little effect on the temporal behaviour of the species.

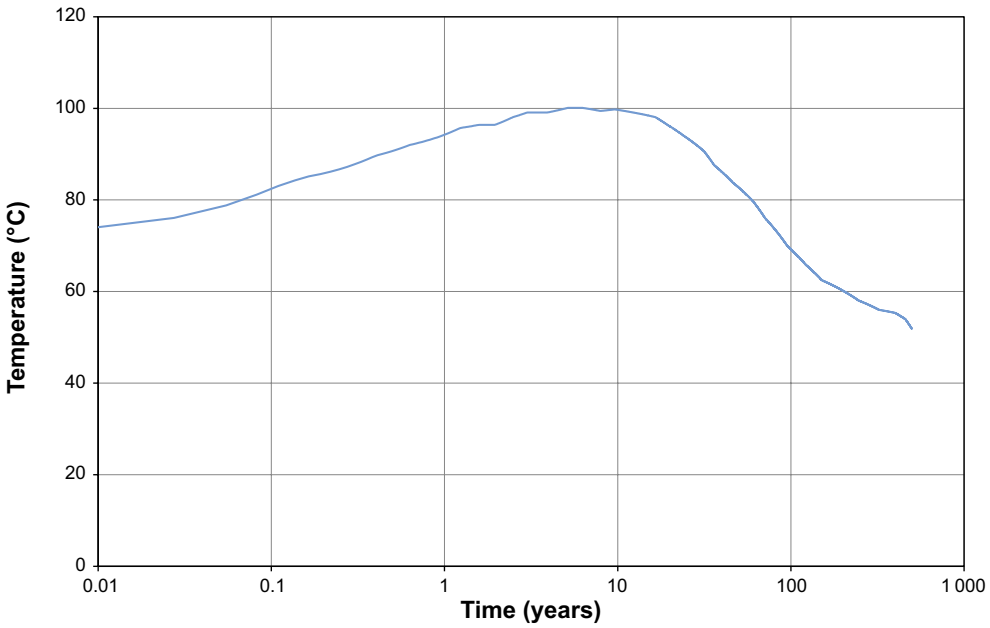

Figure 3-29. *Plot of temperature versus time profile used for Cases 13d and 13e.*

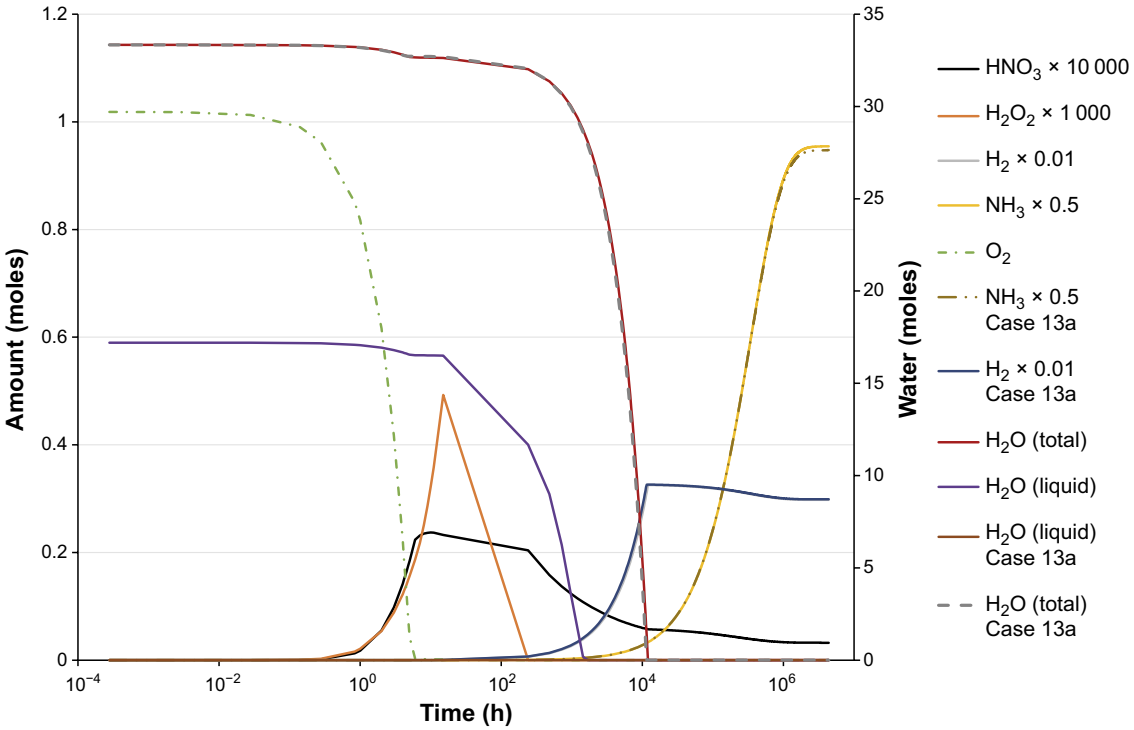

Figure 3-30. *Plot of species amounts versus time for Case 13d. Also plotted are H_2O(liquid), H_2O(total), H_2 and NH_3 for Case 13a.*

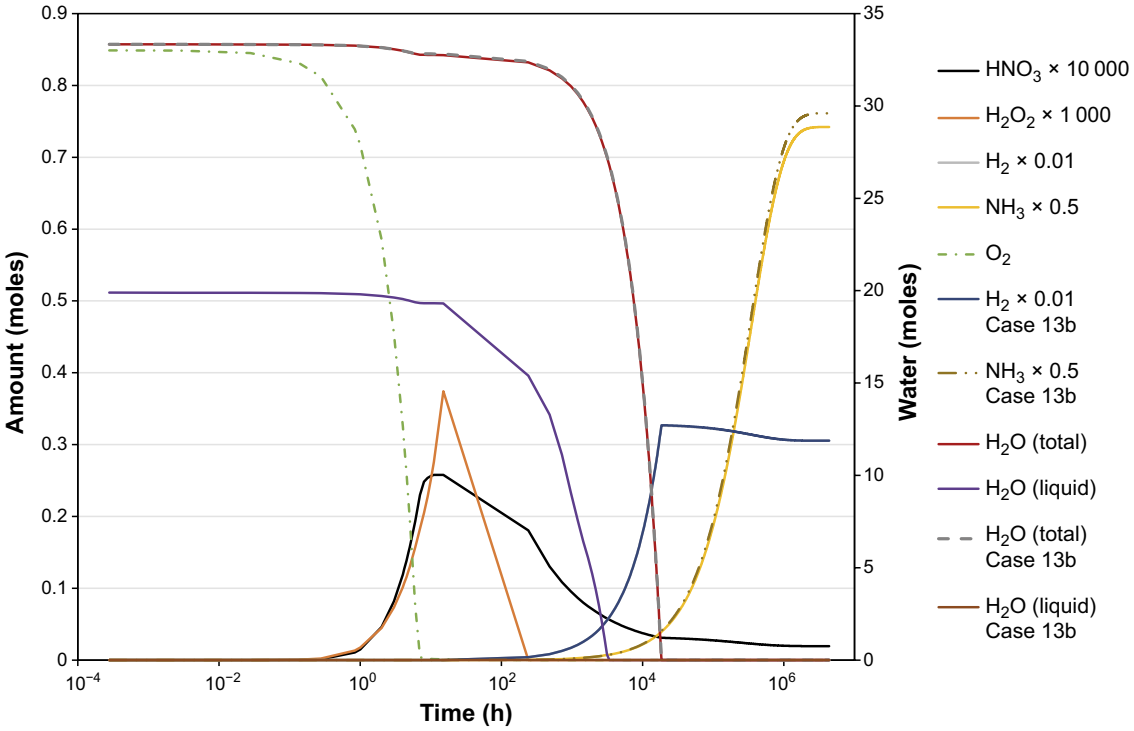

Figure 3-31. *Plot of species amounts versus time for Case 13e. Also plotted are H_2O(liquid), H_2O(total), H_2 and NH_3 for Case 13b.*

3.3.5 Cases 13a, 14, 15, 16 and Cases 17, 18, 19 and 20 – Impact of initial air content

For Cases 13, 14, 15, 16 the initial water in the canister was 600 g but the amount of air present was decreased, 10 %, 5 %, 2 % and 1 %. Cases 17, 18, 19 and 20 are at the same air contents respectively but for 30 g of water in the system. Figure 3-32 is a plot of the steady state amount of ammonia predicted by the model for these 8 cases versus the initial amount of air in the canister.

Comparing Figure 3-32 with the equivalent BWR plot, Figure 3-17, indicates on the whole more ammonia is produced in the PWR Cases. This is likely a consequence of the higher dose rate used for the PWR Cases. The PWR system behaviour is similar to the BWR cases:

- In general, the steady state ammonia amount increases with increasing air content.
- At low water and high air content the ammonia amount starts to fall with increasing air content.
- At low air content the amount of ammonia is greater for the low water cases.

The explanation for these behaviours have been given in Section 3.2.5 for the BWR cases and therefore will not be repeated here.

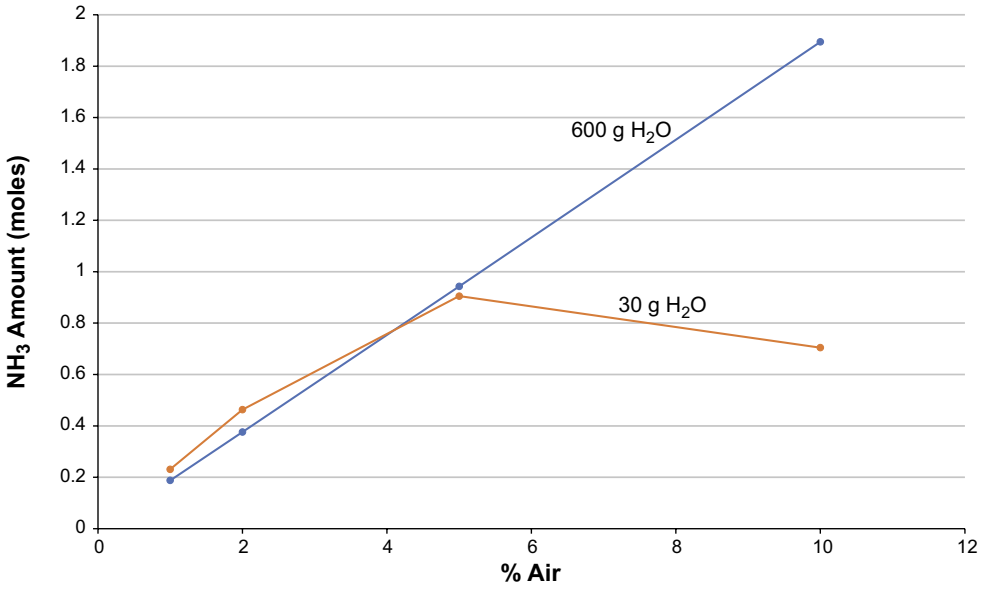

Figure 3-32. *Calculated final amounts of NH_3 for Cases 13a, 14, 15, 16, 17, 18, 19, 20 against initial air content of the canister.*

3.3.6 Cases 21 and 22 – Slow addition of water to the system

The conditions for Case 21 are nominally the same as for Case 14, except the 600 g of water present in the canister is released from the fuel pins slowly at a rate of 1.8 g/day. Figure 3-33 shows the behaviour of O_2, water and both corrosion rates for Case 21. The calculation assumed 1 g of water was present in the system at the start of the calculation.

The plot shows the total water present never gets above 180 g as H_2O is consumed by corrosion. This is primarily anaerobic corrosion as O_2 is consumed by aerobic corrosion within the first 10 h. Therefore, compared with Case 13a, in which the initial amount of water present was 600 g, much less water is experienced in the vapour phase here. However, the total water in the system is significantly more than the equivalent BWR Case 10, this is a result of the smaller surface area for the PWR cases, leading to a slower rate of H_2O consumption by corrosion. When water addition stops at 600/1.8 = 333.33 days (8 000 h) the water in the system is rapidly consumed and anaerobic corrosion stops. Again, it should be noted that no mass transfer limitations are assumed with respect to the corrosion rate, so at low water vapour pressure it is assumed water can arrive at the metal surface fast enough to maintain the corrosion rate.

Figure 3-34 is a plot of species amount for Case 21 and Figure 3-35 is the equivalent plot for Case 22 (30 g of water added over 30/1.8 = 16.7 days).

Note there is no liquid water present in both cases. Comparing these results with the equivalent cases 14 and 18 which contain 600 g and 30 g of water from the start, indicates:

- For 600 g of water adding H_2O gradually leads to a final steady state NH_3 amount less than would be present if the water was present from the start (0.74 moles for gradual addition and 0.85 moles if present at the start). There is still water in the system while ammonia is present.
- For 30 g of water the final steady state NH_3 amount is higher (1.1 moles) if water is added gradually (0.9 moles if water is present at the start). Water has been consumed before ammonia reaches any significant amount for Case 22.

These results along with all the other will be discussed below.

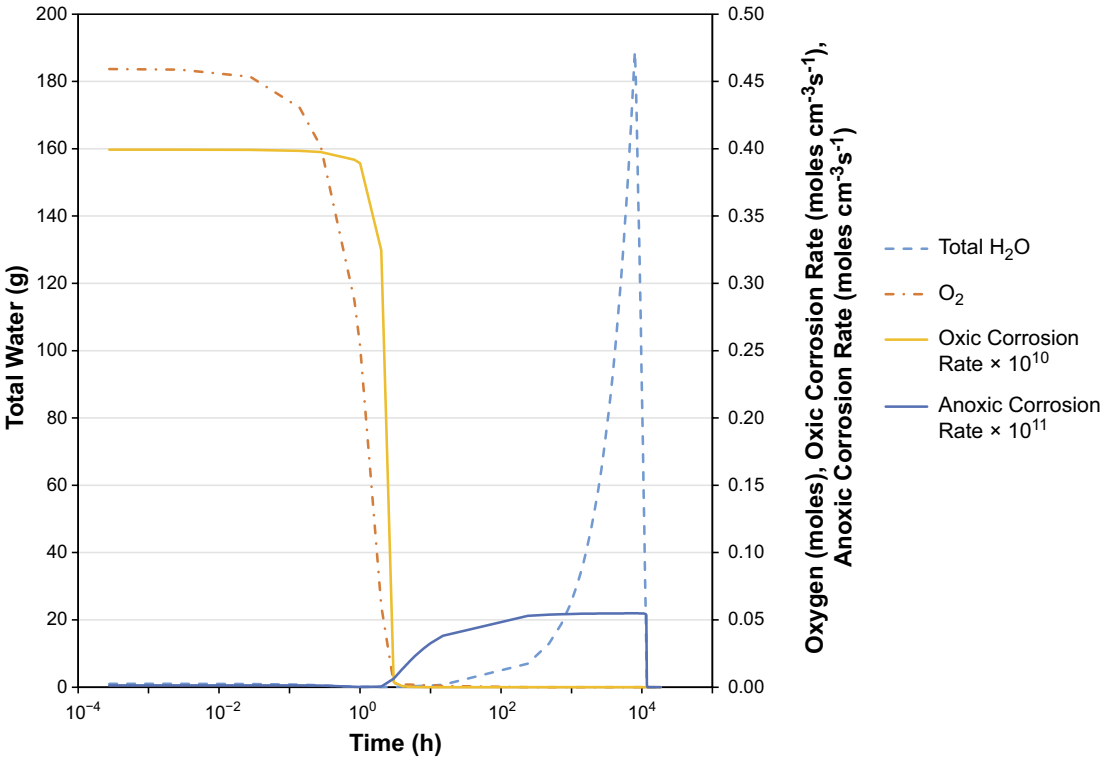

Figure 3-33. *Plot of O_2, total H_2O present, total added H_2O, and rates of aerobic and anaerobic corrosion for Case 21.*

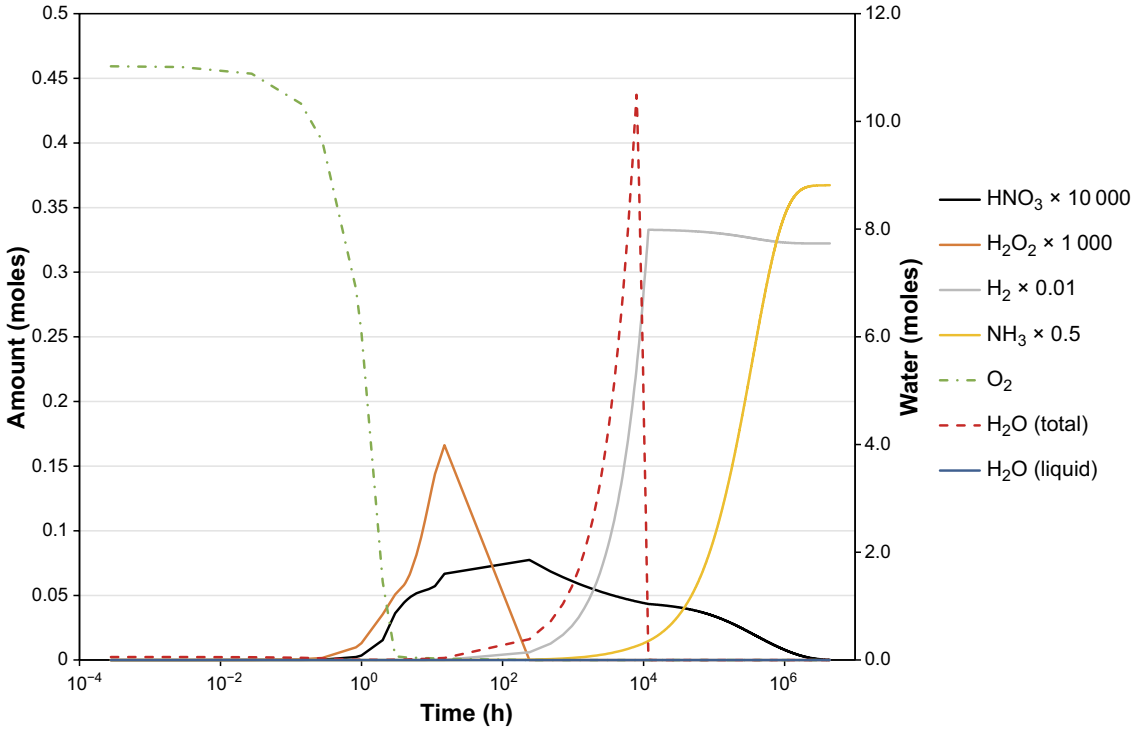

Figure 3-34. *Plot of species amounts versus time for Case 21. There is no liquid water for this case.*

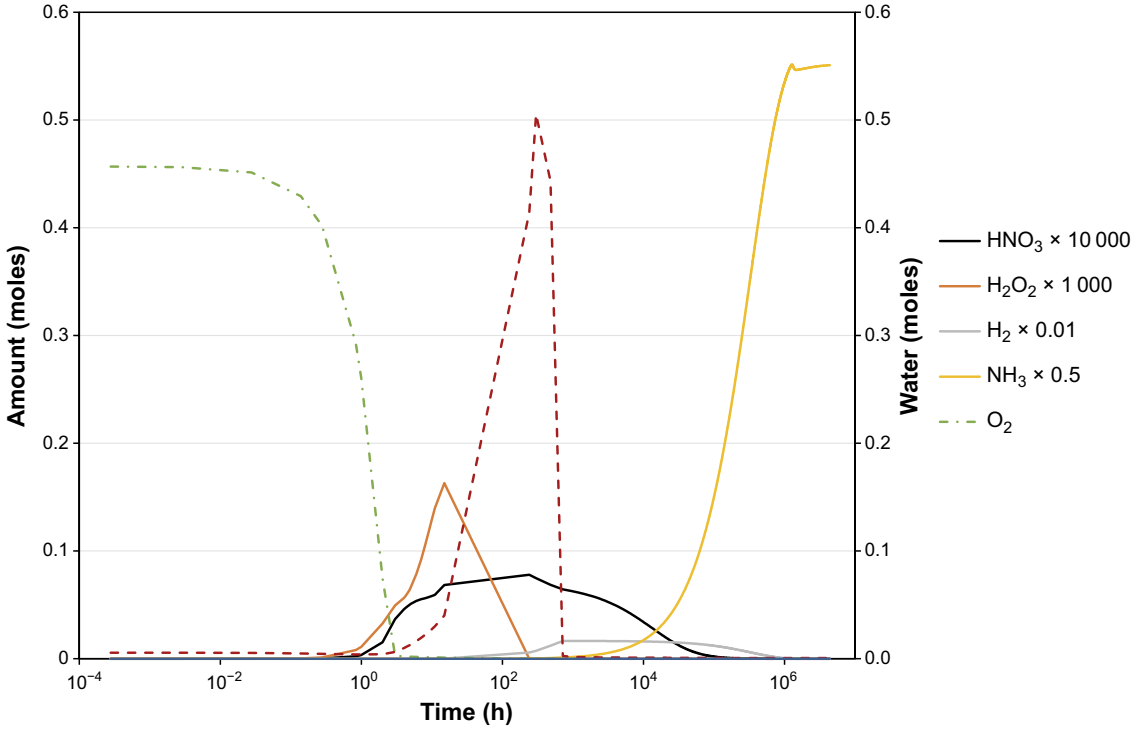

Figure 3-35. *Plot of species amounts versus time for Case 22. There is no liquid water in this case.*

3.4 Cases for zero corrosion rate

Calculations were requested for scenarios in which no corrosion was taking place below a relative humidity of 60 %, these are Cases 10a and 11a for BWR conditions and Case 13f for PWR conditions. From a numerical integration perspective these calculations were particularly difficult to perform, the reasons for which will be discussed here along with the results from the simulations.

The FACSIMILE software (Curtis and Sweetenham 1987) used to solve the simultaneous ordinary differential equations for the problem calculates what is referred to as a Jacobian matrix **J**. The matrix is made up of elements corresponding to the terms $\partial v_i/\partial k_j$, where v_i is a particular variable i (e.g. a gas species concentration) and k_j a particular parameter constant j (e.g. chemical rate constant). The Jacobian **J** is usually sparse (a lot of zero terms) and FACSIMILE uses a number of sparse matrix methods to speed up the simulations. In performing the calculations FACSIMILE needs to calculate the inverse[11] of **J**, i.e. $\mathbf{J}^{-1}$ and to do this it divides a matrix by $|\mathbf{J}|$, the determinant of **J**. The matrix **J** captures the dependencies of all the variables for the problem on all the constants. Problems can arise however if the implementation changes these dependencies during the course of an integration. For the current problem, for example, the gas phase concentration of water (a variable) depends on the radiolysis chemistry (constants equal to G-values and chemical rate constants), evaporation/condensation rate constant, and the corrosion rates (two constants). For the calculations discussed in this section the corrosion rates could be set to zero if RH < 60 % and equal to their normal values if RH ≥ 60 %. However, what this means from a numerical standpoint is that dependencies in **J** that exist on the corrosion rate if RH ≥ 60 %, no longer exist if RH < 60 % or vice versa. This can lead to a row in $|\mathbf{J}|$ becoming a set of zeros and therefore $|\mathbf{J}| = \mathbf{0}$, so that when division by this term is attempted the result is "ill-determined" and the simulation fails. For the present problem this is in fact what occurs if the corrosion rates are simply switched off and on depending whether RH is less than or greater than 0.6. The FACSIMILE language provided a number of commands for tackling these types of problem, which the author of this document has used previously, that allow the user to inform the software the Jacobian "pattern" has changed and outline the new "pattern". However, in the current release of the software used for this work it seems these commands have been disabled, either deliberately by the company that sells the software, or probably, and more likely, inadvertently. The company have been informed of the problem with the software. In order to address the problem therefore another approach was adopted that does not remove the dependencies in the Jacobian matrix completely as RH changes, this is discussed below.

The approach introduces the "pseudo" corrosion rates $'CR$ where:

$$'CR = CR \times F(RH) \tag{3-4}$$

Here CR is the aerobic or anaerobic corrosion rate previously used for the cases above and the function $F(RH)$ is defined as:

$$F(RH) = \exp\left(-\frac{A}{RAMP(RH-B)+C}\right) \tag{3-5}$$

where the RAMP function is defined as:

$$RAMP(RH-B) = \frac{|RH-B|+(RH-B)}{2} \tag{3-6}$$

Thus, for RH < B, RAMP = 0 and for RH > B, RAMP = RH – B. For $A = 10^{-8}$, B = 0.6 and $C = 10^{-9}$ the function in Equation 3-5 is shown in Figure 3-36:

[11] It actually calculates what's referred to as an **LU** decomposition of **J** and performs the inversion on these, but these details are not important.

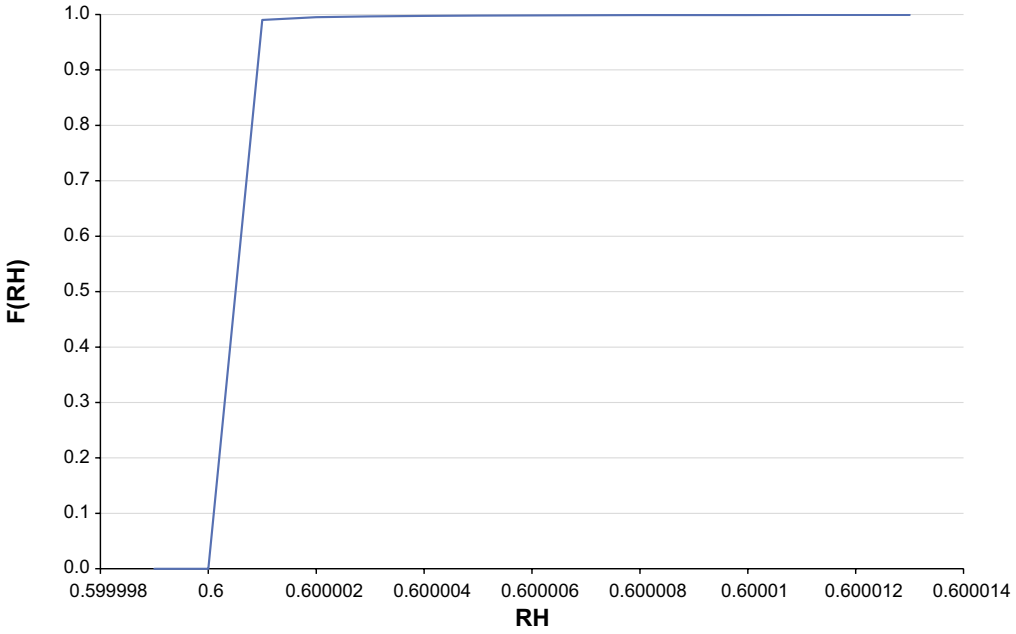

Figure 3-36. *Corrosion rate scaling function against relative humidity (RH as a fraction).*

The function is close to a step function that moves between 0 and 1 as RH (as a fraction) increases/decreases around 0.6. It is though subtly different than an absolute step function, which, as stated above does not work for the current problem. At RH < 0.6 the value of the function is not zero, but it can be made as close to zero as is numerically tolerable by appropriate choices for the parameters A and C. For the example parameters given here the function is of the order of 10^{-5} for RH < 0.6. Likewise, when RH > 0.6 the function doesn't instantaneously become one but approaches one over a finite, although small, range of RH. For the parameter terms A, B and C given here the "pseudo" corrosion rate 'CR moves between 10^{-5} times the normal corrosion rate and the normal corrosion rate as RH transitions from below 0.6 to above 0.6. With these parameter values and the function implemented in the model converged solutions for the Cases 10a, 11a and 13f were obtained, integrating the equations for a canister operational period of 500 years. However, these calculations took several days to complete on a high power laptop, compared to minutes to hours for all the other cases discussed in the report. It is also possible to set the parameters A and C in Equation 3-5 such that the function is $< 10^{-5}$ for RH < 0.6 and changes to 1 over a narrower range of RH above 0.6. One such calculation was performed for Case 13f, choosing A and C parameters so that 'CR was 10^{-10} less than the normal corrosion rate for RH < 0.6. After approximately 14 days the simulation was terminated as it had only reached 100 years of canister operational life and the results were not demonstrating anything significantly different than the results using the parameters that converged faster. There were also several other integration parameters that had to be "tightened" up to get these Cases to converge, the general order of the variable accuracy was changed from 10^{-3} to 10^{-5} (i.e. 3 to 5 significant figures) and the maximum time step size had to be reduced, both of which also impacted the CPU time for the calculations.

3.4.1 Results for BWR Cases 10a and 11a

Case 10a slowly adds water to the system (1.8 g/d) until a total of 600 g has been added. Figure 3-37 shows the species concentrations as a function of time for Case 10a, also plotted is RH. A few points to note:

- Oxygen is consumed, but only after 7 500 h (~0.9 y), compared to 2 h for the equivalent Case 10, as a consequence of the low corrosion rate at RH < 0.6.
- The presence of O_2 in the system for a significantly longer period means that HNO_3 peak amounts are 10^3 times more than for Case 10 and likewise for H_2O_2.
- As soon as O_2 is consumed in the tanks HNO_3 and H_2O_2 are decomposed via radiolysis and NH_3 production increases.
- The behaviour of H_2O and RH is interesting and did not change upon increasing the equation integration accuracy implying the oscillations in RH may be real and not a consequence of numerical issues. As water is added to the system and not consumed by corrosion the relative humidity increases until a value of 0.6 is achieved. Some O_2 is lost prior to RH reaching 0.6 via radiolysis and conversion to HNO_3 and H_2O_2, as is the case for some of the added water. Once RH reaches 0.6 corrosion starts occurring, removing H_2O, which of course will lower RH in the system and halt corrosion. There are therefore several effects occurring in the canister that impact RH: (1) At around 1 to 2 years there are some minor fluctuations in the temperature profile used to model the system (see Figures 3-3 and 3-29) which will cause fluctuations in the equilibrium vapor pressure; (2) Water is being added to the system up to 8 000 h (333 days) potentially increasing RH; (3) Temperature is rising up to approximately 45×10^3 h (~5 y), which will decrease RH, but after this period the temperature falls, which increases RH; (4) Radiolysis chemistry is removing H_2O to form HNO_3, H_2O_2 and lowering RH, but once O_2 is removed from the system HNO_3, H_2O_2 are decomposed by radiolysis, with potential reformation of H_2O, increasing RH; (5) Finally, as stated, corrosion is switching on and off as RH rises and falls below 0.6, with the imposition of corrosion when RH = 0.6 driving RH down and switching corrosion back off. All these processes change with time, probably their relative importance changes also, but a consequence is the complicated calculated behaviour shown in Figure 3-37.
- After 500 years the simulations indicate the canister contains approximately 3 moles of H_2O and ~0.6 moles of NH_3.

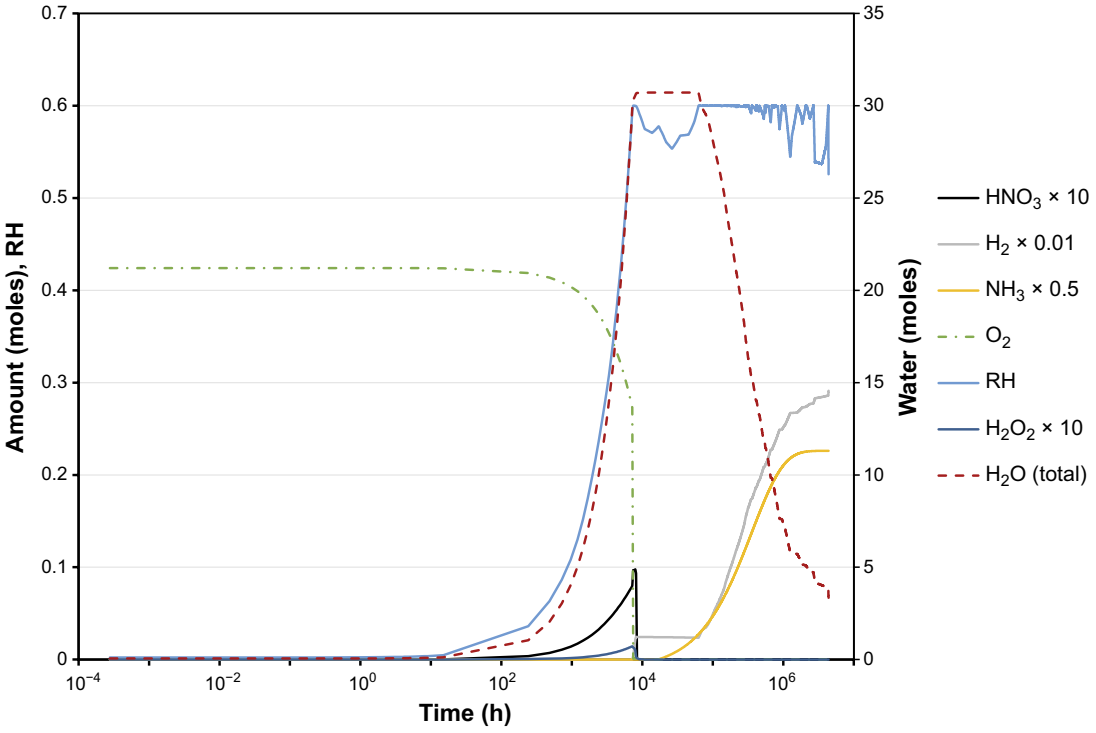

Figure 3-37. *Plot of species amounts versus time for Case 10a.*

For Case 11a only 30 g of water was added gradually to the canister, taking approximately 17 days. The results from this calculation are shown in Figure 3-38.

The behaviour here is simpler than in Case 11a because the RH never achieves 0.6, there is simply not enough water added to the canister. Points to note:

- Both O_2 and H_2O are consumed by corrosion in this calculation but at a corrosion rate ~10^{-5} slower than Case 11. Thus O_2 is consumed after approximately 0.9 y, but water is still present in the system (~0.6 moles) after 500 years.
- RH initially rises as H_2O is added to the canister up to 400 h, after which the increasing canister temperature, occurring up to 4.5×10^4 h, leads to a fall in RH, while beyond this point temperature falls and RH increases. Slow consumption of H_2O by corrosion finally results in a fall in RH towards the end of the 500 y period.
- Compared to Case 11 significant amounts of HNO_3 and H_2O_2 are formed while O_2 is present in the system, but these are removed by radiolysis chemistry once O_2 is consumed by corrosion.
- At 500 y of operation the canister contains mainly NH_3, H_2 and approximately 0.6 (11 g) of water.

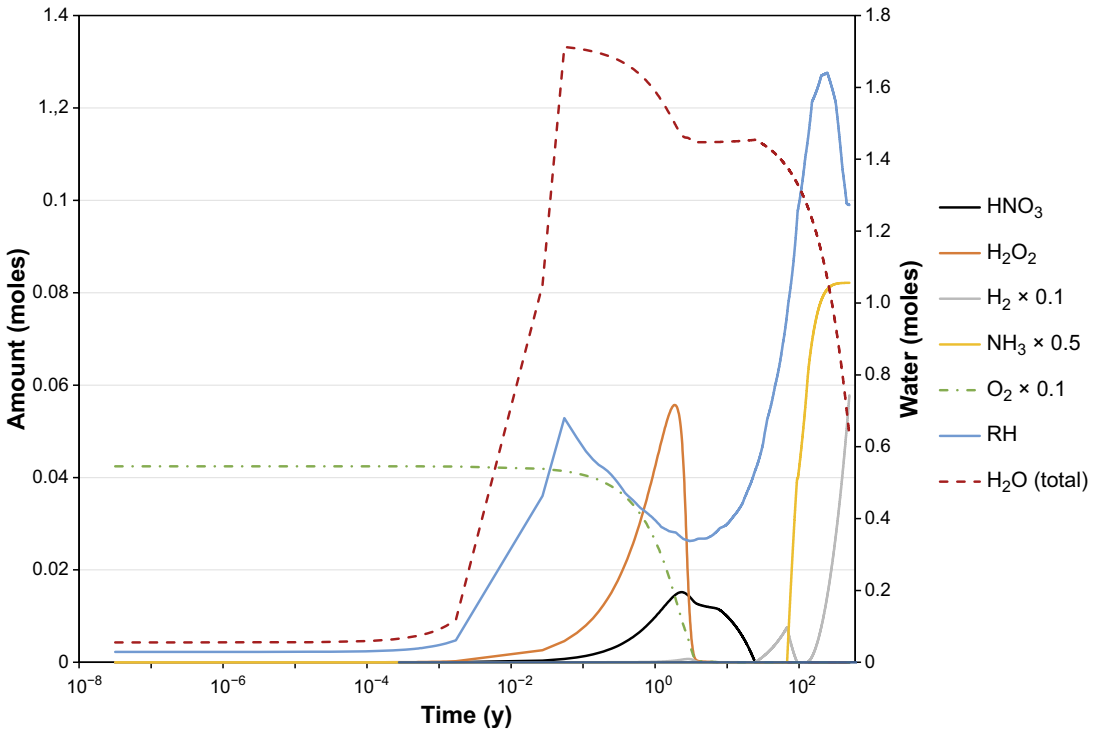

Figure 3-38. *Plot of species amounts versus time for Case 11a.*

3.4.2 Results for PWR Case 13f

Case 13f is based on Case 13a, standard PWR fuel temperature profile, dose rates, areas and volumes with 600 g of water present at the start. The calculation again assumes a corrosion rate of 10^{-5} slower than normal if RH < 0.6. Figure 3-39 shows the simulation results.

Important results from the calculation are:

- With 600 g of water initially present in the canister at a starting temperature of 110 °C the RH is approximately 51 %. This falls as the temperature increases and H_2O is consumed by radiolysis but then starts to rise as the system temperature falls. Analogous to Case 10a oscillations in RH are observed once RH has reached 0.6 and corrosion rates increase by five orders of magnitude. The reasons for these oscillations have already been discussed for Case 10a.
- The amounts of HNO_3 and H_2O_2 formed while O_2 is present is significant, with peaks close to 0.3 and 0.5 moles respectively, roughly 10^4 times larger than for Case 13a. These species are rapidly decomposed by radiolysis once RH = 0.6 and the final amounts of O_2 are removed by corrosion.
- At the end of the 500 y operational period the predominant gases in the system are H_2 and NH_3 with approximately 4 to 5 moles of water still present in the system.

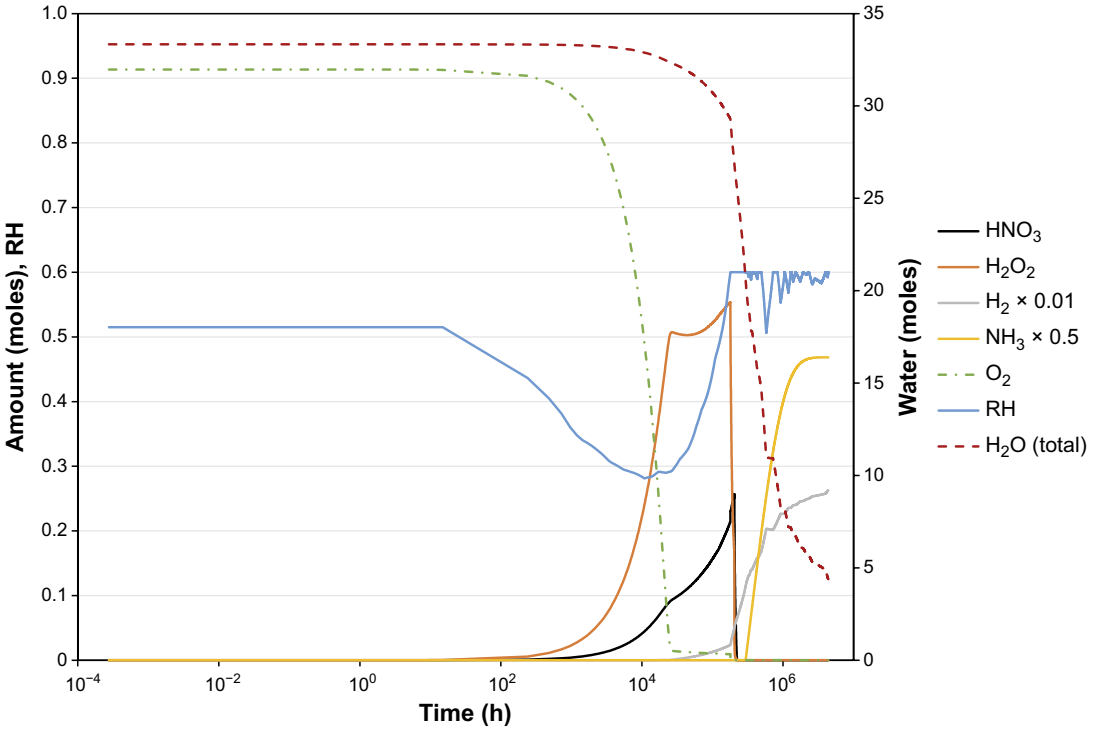

Figure 3-39. *Plot of species amounts versus time for Case 13f.*

3.5 Application of the model to graphite gasket/Seal degradation

The model so far has been used to investigate the amounts of aggressive gas phase species that may be present in the canister important to metal alloy corrosion. Both nitric acid and ammonia may lead to localised corrosion phenomena in steel and copper alloys and so the focus of the model has been on the amounts of these species and on the time-scale of their formation. However, during the course of this study the question arose as to whether radiolytic produced species may also cause degradation problems of non-metallic components. In particular, might gas phase radiolysis products impact the graphite gasket used to seal the lid of the carbon steel insert? This is in place to prevent gas transfer between the insert interior and the copper overpack. A brief investigation of this process was therefore performed and is reported here.

Graphite is stable in air and does not oxidise under normal ambient conditions. However, in the presence of radiation it is oxidised in gases containing oxygen (see Davidge et al. 1959). To estimate the oxidation rate of the graphite gasket and corresponding generation rate of CO_2 in the gas phase it is necessary to appreciate the oxidation mechanism of graphite in an irradiated gas containing oxygen. This will not be discussed in detail here, but a great deal of work on this topic has been carried out with regard to the graphite moderator in an Advanced Gas Cooled Reactor (AGR) (for example see Best et al. 1985). In these systems the coolant is primarily CO_2, but also CO, H_2O, H_2 and CH_4 are present in significant quantities. The gas phase radiation chemistry of these components leads to a selection of potentially oxidising species in the coolant: O, O_2, O_3, OH, H_2O_2, along with more obscure species such as CO_3^- (see Leary et al. 2000). The mechanism for oxidation is the adsorption of an oxidising species on the basal plane of the graphite, its surface diffusion to the edge of the basal plane, followed by reaction with edge C atoms and loss of CO or CO_2 into the gas phase. That is, oxidation is "nibbling away" of the carbon planes at their edges in graphite. There is good experimental evidence for this mechanism. A key question regarding this mechanism is which oxidising species, one or several, of those present actually performs the oxidation. Quantum mechanics calculations indicate only O atoms and CO_3^- actually adsorb on the graphite basal plane, indicating species such as O_2, OH etc do not oxidise the material directly (Leary et al. 2000, Incze et al. 2003). Examination of the gas phase radiation chemistry in the AGR systems indicates the concentration of O atoms is several orders of magnitude larger than CO_3^-, therefore the most likely oxidising species is O atoms. It should be noted that in AGRs the radiation dose rates are many orders of magnitude larger than in the KBS-3 canister and the operating temperatures can be as high as 700 °C yet the oxidation of graphite is still very slow. The design life of the AGR graphite moderator was 25 years and many of these reactors are still operational after almost 50 years with a functioning moderator. It should be expected therefore that the radiolytic oxidation of the graphite gasket in the KBS-3 canister will be very slow and the simple analysis below demonstrates this.

In the canister the presence of air and water will lead to the production of various oxidising species: O, O_2, O_3, OH, H_2O_2 and perhaps some associated with nitrogen. However, it is likely in this system that O atoms will be the primary species oxidising any graphite type materials present, as in the AGR. The analysis here will make this assumption and to get an estimate of the gasket corrosion rate it is necessary to know the amounts of O atoms in the canister and the rate of delivery of these atoms to the gasket surface.

The KBS-3 canister radiolysis model predicts the concentration of O atoms for Case 13a (600 g H_2O, 10 % air) shown in Figure 3-40.

The oxygen atom concentration starts at around 1.7×10^{-15} moles cm^{-3} and rapidly drops by two orders of magnitude in a matter of hours. Although not plotted, as the system evolves over long periods of time the concentration of O gets smaller.

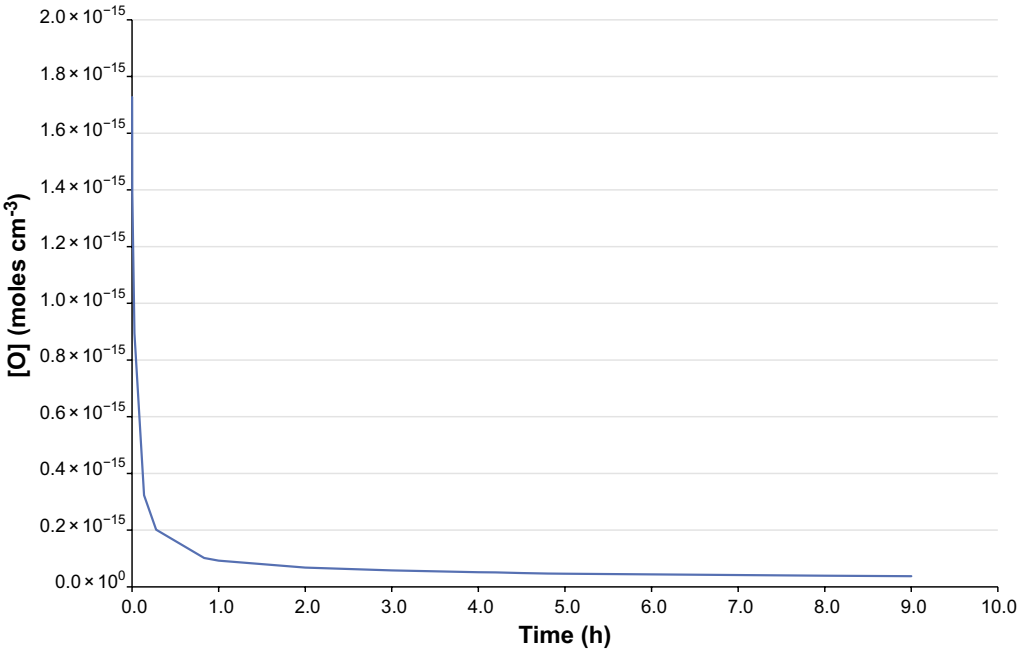

Figure 3-40. *Oxygen atom concentration against time for Case 13 (PWR conditions, 600 g H_2O, 10 % air).*

To calculate the rate of delivery of O atoms to the surface it is necessary to estimate the mass transfer rate to the surface. In a perfectly homogeneous system this will only occur by diffusion, but the canister is not homogeneous and different temperatures exist within the container depending on location. It is highly likely then that convective flow will be occurring in the gas during storage and this will greatly increase mass transfer rates compared to simple diffusion. To estimate what this mass transfer rate is, the correlation developed by El-Riedy (1981) for mass transfer under natural convection was used. El-Riedy gives the following expression for the Sherwood number for mass transport controlled by natural convection:

$$Sh = 0.59(GrSc)^{0.25} \tag{3-7}$$

Where the Sherwood number is defined by:

$$Sh = \frac{k_m \delta}{D} \tag{3-8}$$

Here k_m is the mass transport rate, δ is the characteristic length and D is the diffusion constant of the species. Gr is the Grashof number, defined as:

$$Gr = \frac{g \Delta\rho \delta^3}{\nu^2 \rho} \tag{3-9}$$

where g is the acceleration due to gravity (9.8 $m^2\ s^{-1}$), Δρ is the density difference due to the temperature difference, ρ the average density of the gas and ν is the kinematic viscosity, defined by:

$$\nu = \frac{\mu}{\rho} \tag{3-10}$$

where μ is the viscosity of the fluid. The Schmidt number (Sc) and is given by:

$$Sc = \frac{\nu}{D} \tag{3-11}$$

where D is the diffusion constant of the species in the medium.

To estimate the quantities involved parameters for CO_2 were used, although it is recognised here we are concerned with the transport of O primarily in Ar gas. The quantities for CO_2 were readily available and should provide a reasonable estimate of the order of magnitude of the numbers involved. If required, then parameters for O and He can be obtained and used later to provide more accurate values for the calculations. To determine the various non-dimensional numbers for the gas the following properties were used:

Density of gas (kg m^{-3}) $\rho = MW_{CO2}\frac{P}{RT}10^{-3}$ (3-12)

Viscosity of CO_2 (Pa s) $\mu = 18.27 \times 10^{-6}\frac{291.15 + 120}{T + 120}\left(\frac{T}{291.15}\right)^{3/2}$ (3-13)

Diffusion constant for CO_2 in air (m^2 s^{-1}) $D = 1.6 \times 10^{-6}\left(\frac{T}{298}\right)^{3/2}$ (3-14)

where T is the temperature in kelvin. Table 3-3 gives physical parameters assumed for the calculation.

Table 3-3. Lists parameter values used in mass transport calculation.

Parameter	Value
Volume (m^3)	1.448
Characteristic Length (m)	1.13
Temperature Difference ΔT (°C)	10
Pressure (Pa)	105
C Atom Interatomic Spacing (nm)	0.147
Graphite Basal Plane Spacing (nm)	0.335
Exposed area of Graphite Gasket (cm^2)	80

With the above equations and input parameters the mass transfer rate calculated using the El-Riedy correlation was 3.8×10^{-4} ms^{-1}. If it is assumed an O atom concentration equal to the maximum from the radiolysis calculation shown above for Case 13a, 1.7×10^{-15} moles cm^{-3}, exists throughout operations, then this gives a flux of O atoms towards the gasket surface of $J = k_m[0] = 3.9 \times 10^{11}$ atoms m^{-2} s^{-1}. Since the surface area of the gasket is $A = 80 \times 10^{-4}$ m^2, this means a maximum removal rate from the gasket of C atoms of JA, which is equal to 3.1×10^9 C atoms/s, assuming 1 adsorbed O atom removes 1 C atom. The number of atoms on the graphite basal plane is roughly $1/(0.147 \times 10^{-9})^2 = 4.6 \times 10^{19}$ m^{-2}, so on the top surface of the gasket this will mean there are 4.6×10^{19} $m^{-2} \times 80 \times 10^{-4}$ m^2 atoms = 3.7×10^{17} atoms. If these are removed at 3.1×10^9 C atoms/s, as estimated here, it will take 3.8 years to remove the top layer of atoms. This is equivalent to an oxidation rate of 9×10^{-2} nm/year, i.e. very small. The oxidation process generates 3.1×10^9 C atoms/s in the gas phase or 3.6×10^{-21} moles cm^{-3} s^{-1} of CO or CO_2. This amounts to 1.1×10^{-13} moles cm^{-3} generated after 1 year. This should be compared with the amount of CO_2 likely to be present in the canister at the start, which for 10 % air, assuming 0.04 % CO_2 in air, amounts to 1.3×10^{-7} moles cm^{-3}. The amount of CO/CO_2 generated by corrosion of the gasket is tiny compared to what would be present initially.

It has been assumed here that the O concentration remains at 10^{-15} moles cm^{-3} when in fact it falls dramatically within a few hours. The rates of gasket corrosion and CO/CO_2 generation given here are therefore over estimates of the likely values. However, even with this assumption the corrosion rates and CO/CO_2 production rates are insignificant.

4 Discussion

This report describes a model of the radiolysis chemistry taking place in the gas phase of the KBS-3 canister. This gas phase chemistry can lead to aggressive reagents such as HNO_3 and NH_3 that can cause localised corrosion phenomena in steel and copper materials used to construct the canister. An earlier report by Henshaw and Spahiu (2021) gives the details of the model, along with the results of validation calculations and the application of the model to the KBS-3 canister. The model in addition to simulating the gas phase radiolysis chemistry also accounts for the impact of corrosion on this chemistry and the evaporation/condensation of water in the system.

Since the 2021 report by Henshaw and Spahiu, different design parameters for the KBS-3 canister have been suggested, affecting accessible surface areas, gas space volumes for the system, dose rates to the gas and potential temperatures within the vessel. It was therefore considered necessary to re-asses the chemistry within the canister using the revised input conditions.

Chapter 3 describes the revised scenarios that have been examined with the model along with the results from the calculations. Table 4-1 summarises the cases and results. In total 34 cases have been modelled roughly half of which consider a canister containing BWR fuel and half containing PWR fuel. The impact of changing dose rate, air content, water content, temperature, corrosion rate, available surface area and volume have been examined. The amounts of species generated in the canister predicted by the model have been presented in Chapter 3. For most of the cases O_2 is consumed by corrosion relatively rapidly (tens of hours) and the prevailing long-term conditions in the canister are reducing with excess H_2 present. This means the major long-term gas products are H_2 and NH_3 produced from radiolysis of N_2 present from air contamination. For most of the cases in Table 4-1 the amounts of HNO_3 present were small, of the order of 10^{-5} moles or less, compared to amounts of NH_3 which are of the order of moles. This situation is not the case for those scenarios in which very low corrosion rates were assumed if RH was less than 0.6. For these cases, 10a, 11a and 13f, significant amounts of HNO_3 and H_2O_2 are formed while O_2 is present, but are removed once O_2 is consumed by corrosion. For these cases the predicted final products after 500 y are mainly H_2 and NH_3, with H_2O still present in the system. From the results in Table 4-1, and those discussed in Chapter 3, a number of observations can be made:

- Significant liquid water only exists in the system for the BWR Cases 1–5, for the other cases either the total amount of water in the system is too low to form a liquid phase or the system temperature is too high and the saturation pressure of water is therefore high. For Cases 1–5 liquid water is lost around 480 h and the amount of NH_3 in the system at this point is between 10^{-4} and 10^{-3} moles, so small.
- The larger the dose rate to the gas the larger the amount of NH_3 produced in the system. This is apparent in comparing the BWR cases 1 and 2a as well as the PWR cases 12 and 13a. In addition, the higher the dose rate the sooner NH_3 starts to be produced. This is apparent from Table 4-1, for example, in that to reach 10^{-3} moles of NH_3 in the system takes 60 days for Case 1 (BWR low dose rate) but only 20 days for Case 2a (BWR high dose rate).[12]
- Generally, changes in temperature do not impact the results significantly. Comparing PWR Cases 13a and 13d, where calculations for 13d were performed at a lower temperature, the final steady state amounts of NH_3 were similar, 1.90 and 1.91 moles respectively. The time to achieve 10^{-3} moles of NH_3 increased from 10 to 20 days upon lowering the temperature, implying a slower formation rate of NH_3. At the expected PWR temperature conditions the initial relative humidity in the system was 51 %, for an initial water content of 600 g, so high relative humidity and high NH_3 amounts cannot occur. Of course, when the temperature is dropped, the relative humidity increases, and in Case 13e 0.03 moles of NH_3 is present in the system when the humidity has fallen from 100 % to 60 % (Case 13e, Table 4-1. Note Case 13e is analogous to 13d but with a lower system volume and surface area.).

[12] An arbitrary value of 10^{-3} moles was chosen to provide a relative rate of production for the various cases.

- Lowering the available surface area for corrosion and system volume leads to less NH_3 production. This is apparent from comparing the steady state amounts of NH_3 for Cases 2a and 2b (BWR fuel) and Cases 13a and 13b (PWR fuel). The time evolution of NH_3 production is not impacted significantly.
- Increasing air content generally leads to larger amounts of NH_3 produced. However, the behaviour depends on the water content (see Figures 3-17 and 3-31) and results for Cases 3–9 (BWR) as well as Cases 14–20 (PWR) listed in Table 4-1. At low water content the limited supply of H_2 sets limits on the amount of NH_3 that can be produced, so increases in air present can actually lead to a fall in the amount of ammonia produced, the reason for which is discussed in Chapter 3.
- Decreasing the corrosion rates does not have a large impact on the steady state amounts of NH_3 produced (see Cases 2b and 2c (BWR) as well as Cases 13b, 13c (PWR) in Table 4-1). What it does affect though is the period of time that H_2O exists in the system. For Cases 13b and 13c (low corrosion rate) an order of magnitude fall in corrosion rate increases this time from 771 to 7 710 days. When water is lost from the system for Case 13b, only 8×10^{-2} moles of NH_3 are present in the canister, but for Case 13c 0.6 moles exist, so water and ammonia co-exist for longer at the lower corrosion rate.
- The impact of allowing water to be added gradually to the system can be seen from comparing the results from Cases 10 and 11 with Cases 3 and 7 (BWR), as well as comparing Cases 21 and 22 with Cases 14 and 18 (PWR). In the BWR case adding H_2O gradually leads to a decrease in steady state NH_3 amounts, 0.59 moles (Case 3) compared to 0.47 moles (Case 10), 0.79 moles (Case 7) versus 0.74 moles (Case 11). For the PWR case this is also true at high water content, 0.94 moles (Case 14) versus 0.73 moles (Case 21) but not at low water content, 0.9 moles (Case 18) versus 1.1 moles (Case 22). It has already been discussed that varying the amount of water in the system as well as simply changing the concentration of H_2O present in the gas space also changes how the radiation dose rate is partitioned amongst the main gas constituents. For example, less water present relative to N_2 means a larger fraction of the radiation interacts with N_2, a major step in NH_3 production, which tends to increase NH_3 production. However, less water can lead to less H_2 resulting in less NH_3. Which of these opposing behaviours dominate will depend on the rate of production of H_2 (depending of surface area) and possibly temperature (gas kinetics), so simple trends in behaviour may or may not be expected, as observed in the BWR cases but not the PWR cases.
- The complicated behaviour of the system discussed above is also reflected in the results when comparing the amounts NH_3 produced in the BWR cases with those for PWR fuel. At high water content there is clearly more NH_3 produced for the PWR cases (compare Case 2a (BWR) 1.17 moles NH_3 with Case 13a (PWR), 1.9 moles of NH_3). At low water content the difference is not so clear (compare Case 6 (BWR) 0.73 moles NH_3 with Case 17 (PWR), 0.7 moles of H_2O.
- Two of the worse-case scenarios considered here are Cases 2c and 13c, both using low corrosion rates. For Case 2c the amount of NH_3 increases above 10^{-3} moles after 20 days, but water remains in the system up to 3 200 days, while for Case 13c NH_3 is above 10^{-3} moles after 30 days and water is eventually consumed at 7 708 days. However, for Case 2c the relative humidity has fallen to <60 % after 130 days and for Case 13c it starts at 51 % and falls.
- If very slow corrosion occurs below a relative humidity of 60 % this potentially can have a large impact on the conditions within the canister. Cases 10a, 11a and 13f investigate this behaviour. Slow corrosion means oxygen is present in the gas phase for longer leading to significant amounts of HNO_3 and H_2O_2, peak values 10^4 larger than when relative humidity is assumed to have no effect on corrosion. The system does eventually become reducing, with little HNO_3, H_2O_2 and predominantly NH_3 and H_2 present, but this takes significantly longer to achieve. Comparing Cases 13a and 13f in Table 4-1, for example, the time it takes to obtain 10^{-3} moles of NH_3 increases from 10 days to approximately12 000 days. Also for all the cases in which corrosion is low for a RH less than 60 % water is still present in the system after 500 years of operation.

Table 4-1. List of cases and summary results from the model. (CR – Corrosion Rate, RH-Relative Humidity, † – Never acheived a RH of 60 %).

Case	Description	Steady State NH_3 (moles)	Steady State H_2 (moles)	Time for H_2O to be consumed (days)	Time to acheive 60 % RH (days)	Time NH_3 to reach 0.001 mole (days)	Amount of NH_3 at 60 % RH (moles)	Amount of NH_3 at zero H_2O (moles)
1	BWR low dose rate	0.29	32.3	300.0	80	60.0	1.50E–03	5.60E–03
2a	BWR base case, 600 g H_2O	1.17	30.9	320.0	80	20.0	6.40E–03	2.60E–02
2b	BWR low SA and vol., 600 g H_2O	0.88	31.6	410.0	130	20.0	7.80E–03	2.40E–02
2c	BWR Low SA and vol., 600 g H_2O, low CR	0.88	31.6	3200.0	130	20.0	7.80E–03	1.70E–01
3	BWR, 600 g H_2O, 5 % air	0.59	33	320.0	80	30.0	3.20E–03	1.20E–02
4	BWR, 600 g H_2O, 2 % air	0.23	32.9	320.0	80	70.0	1.30E–03	5.10E–03
5	BWR, 600 g H_2O, 1 % air	0.17	33.1	320.0	80	130.0	6.30E–04	2.60E–03
6	BWR base case, 30 g H_2O	0.73	8.0E–07	20.0	†	20.0		1.90E–03
7	BWR , 5 % air, 30 g H_2O	0.79	0.2	20.0	†	30.0		4.30E–04
8	BWR, 2 % air, 30 g H_2O	0.31	1.1	20.0	†	50.0		3.90E–04
9	BWR, 1 % air, 30 g H_2O	0.16	1.38	20.0	†	100.0		1.90E–04
10	BWR, 1.8 g/d injection, 5 % air, 600 g H_2O	0.47	32.6	340.0	†	30.0		1.40E–02
10a	BWR, 1.8 g/d injection, 5 % air, 600 g H_2O, CR low for RH < 0.6	0.32	1	> 500 y	2600	729	2.7E–2	N/A
11	BWR, 1.8 g/d injection, 5 % air, 30 g H_2O	0.74	0.5	20.0	†	20.0		8.80E–04
11a	BWR, 1.8 g/d injection, 5 % air, 30 g H_2O, CR low for RH < 0.6	0.16	0.58	> 500 y	N/A	25200	N/A	N/A
12	PWR, low dose rates	0.5	32	479.2	†	40.0		1.50E–02
13a	PWR base case, 600 g H_2O	1.9	29.9	479.2	†	10.0		6.40E–02
13b	PWR low SA and vol., 600 g H_2O	1.52	30.5	770.8	†	20.0		8.20E–02
13c	PWR low SA and vol., 600 g H_2O, low CR	1.52	30.5	7708.3	0.625	30.0	0	6.30E–01
13d	PWR, 600 g H_2O, low temp.	1.91	29.8	508.3	180	20.0	2.40E–02	6.80E–02
13e	PWR, 600 g H_2O, low temp., low SA and vol.	1.48	30.5	770.8	320	20.0	3.40E–02	7.90E–02
13f	PWR base case, 600 g H_2O, CR low for RH < 0.6	0.94	26.3	> 500 y	7460	12295	10^{-29}	N/A
14	PWR, 600 g H_2O, 5 % air	0.94	31.6	491.7	†	20.0		3.30E–02
15	PWR, 600 g H_2O, 2 % air	0.38	32.6	491.7	†	40.0		1.30E–02
16	PWR, 600 g H_2O, 1 % air	0.19	33	491.7	†	80.0		6.60E–03
17	PWR base case, 30 g H_2O	0.7	9.0E–07	20.0	†	10.0		1.40E–03
18	PWR, 5 % air30 g H_2O	0.9	5.0E–06	30.0	†	20.0		2.50E–03
19	PWR, 2 % air30 g H_2O	0.46	0.85	30.0	†	40.0		9.90E–04
20	PWR, 1 % air30 g H_2O	0.23	1.26	30.0	†	60.0		4.90E–04
21	PWR, 1.8 g/d injection, 5 % air, 600 g H_2O	0.73	32.2	491.7	†	20.0		2.90E–02
22	PWR, 1.8 g/d injection, 5 % air, 30 g H_2O	1.1	8.0E–07	30.0	†	20.0		2.30E–03

The model has also been used to investigate the oxidation of the graphite seal in the system by the radiolysis products in the gas. The conclusion presented is that this will be very slow, of the order of 9×10^{-11} m/year. That is, it would take 10^4 years to oxidise 1 mm of the seal. This is to be expected, given oxidation of graphite in high temperature gas reactors where the radiation dose rates and temperatures are much higher is known to be slow.

5 Summary

This report discusses the application of the KBS-3 gas phase radiolysis model to predict the long-term gas composition in the KBS-3 canister. Cases have been investigated for both BWR and PWR fuel. The conclusions from the work are that:

- Long term redox conditions inside the canister will be reducing, with NH_3 and H_2 being the primary components produced from radiolysis.
- The amounts of NH_3 and H_2 in the system is a function of the initial amounts of H_2O and air.
- Increasing air at high water content leads to increased amounts of NH_3, but at low water content the amount of NH_3 in the system may decrease with increasing air content.
- Increasing dose rate leads to increased amounts of NH_3 present in the system.
- The available area for corrosion and the free gas volume in the system also impact the amount of NH_3 formed.
- For some of the scenarios investigated here NH_3 and H_2O exist simultaneously in the system, but at high relative humidity (> 60 %) the amount of NH_3 present is small.
- The length of time H_2O is present in the system is largely determined by the anaerobic corrosion rate. This therefore impacts the length of time NH_3 and H_2O exist simultaneously in the system, with low corrosion rates extending the period of time.
- If corrosion rates are low for low relative humidity (< 60 %), then oxygen is present in the system for longer and significant amounts of HNO_3 and H_2O_2 can be formed, but are destroyed by radiolysis once O_2 is consumed.
- Corrosion of the graphite seal used in the canister by gas radiolysis products will be very slow.

The model does not calculate the amounts of species in solution as the system evolves and water is present, as it does not account for liquid-gas partitioning of species such as NH_3, HNO_3 etc.

6 Acknowledgements

The authors would like to thank SKB for sponsoring this work and Kastriot Spahiu for his help and support during the project.

References

SKB's (Svensk Kärnbränslehantering AB) publications can be found at www.skb.com/publications. SKBdoc documents will be submitted upon request to document@skb.se.

Curtis A, Sweetenham W, 1987. FACSIMILE User's Manual. Report AERE-R12805, Harwell Laboratory, UK.

Davidge P C, Tomlinson M, Wright J, 1959. The oxidation of graphite during irradiation in oxygen. UKAEA report AERE C/R 1450, United Kingdom Atomic Energy Authority.

Henshaw J, Hoch A and Sharland S, 1990. Further assessment of the Advanced Cold Process Canister. AEA-D&R report 0060, United Kingdom Atomic Energy Authority.

Henshaw J, 1994. Modelling nitric acid production in the ACPC due to irradiation of moist air. SKB TR-94-15, Svensk Kärnbränslehantering AB.

Henshaw J, K Spahiu K, 2021. Radiolysis Calculations of Air, Argon and Water Mixtures in a KBS-3 Canister. SKB report TR-21-11, Svensk Kärnbränslehantering AB.

Lapuerta S, Bérerd N, Moncoffre N, Millard-Pinard N, Jaffrézic H, Crusset D, Féron D, 2008. The influence of relative humidity on iron corrosion under proton irradiation. Journal of Nuclear Materials, 375, 80–85.

Leary P, Ewels C P, Heggie M I, Jones R, Briddon P R, 2000. Modelling Carbon for Industry: Radiolytic Oxidation, Physica Status Solidi, 27, 429.

Incze A, Pasturel A, Chatillon C, 2003. Oxidation of graphite by atomic oxygen: a first-principles approach. Surface Science, 537, 55.

Loberg J, 2023. Canister dose calculations. SKB R-22-08, Svensk Kärnbränslehantering AB.

Marsh G, 1990. A preliminary assessment of the Advanced Cold Process Canister. AEA Technology. Report AEA-InTec-0011, AEA Technology, UK.

Neretnieks I, and Johansson A J, 2014. Corrosion of the copper canister inside due to radiolysis of remaining water in the insert. SKBdoc 1419961 ver 1.0, Svensk Kärnbränslehantering AB.

El-Riedy M K, 1981. Analogy between heat and mass transfer by natural convection from air to horizontal tubes. International Journal of Heat and Mass Transfer, 24, 365–369.

Ronneteg U, 2023. Version 4.0 av 1939700 KBP3021 REBUS – Input parameters post-closure safety – Concept 1. SKBdoc 2026552 ver 1.0, Svensk Kärnbränslehantering AB.

Samie F, Tidblad J, Kucera V, Leygraf C, 2007. Atmospheric corrosion effects of HNO3 – Influence of temperature and relative humidity on laboratory-exposed copper. Atmospheric Environment 41, 1374–1382.

SKB 2006. Long-term safety for KBS-3 repositories at Forsmark and Laxemar – a first evaluation. Main report of the SR-Can project. SKB TR-06-09, Svensk Kärnbränslehantering AB.

SKB 2010. Design, production and initial state of the canister. SKB Technical Report TR-10-14, Svensk Kärnbränslehantering.

Spahiu K, 2021. Residual water and gases in a KBS-3 canister and their effect on post-closure safety. SKB TR-21-12, Svensk Kärnbränslehantering AB.

Arkitektkopia AB, Bromma, 2023

SKB is responsible for managing spent nuclear fuel and radioactive waste produced by the Swedish nuclear power plants such that man and the environment are protected in the near and distant future.

skb.se